



Original Research Article

## Phytoconstituents of *Chromolaena odorata* (L.) leaf extract for the synthesis of copper oxide/copper nanoparticles and evaluation of their biological potential in wound healing

SOBHA KOTA<sup>1</sup>✉, PRADEEP DUMPALA<sup>1</sup>, RADHIKA SAJJA<sup>2</sup>, AND RATNAKUMARI ANANTHA<sup>1</sup><sup>1</sup>Department of Chemical Engineering, RVR & JC College of Engineering, Guntur 522019, Andhra Pradesh, India<sup>2</sup>Department of Mechanical Engineering, RVR & JC College of Engineering, Guntur 522019, Andhra Pradesh, India

### ABSTRACT

*Chromolaena odorata* (L.), locally named Siam weed, is a rich source of phyto-bioactives and has been traditionally used for wound healing. This study deals with the phytochemical investigation of the leaves of *C. odorata* (L.) for their antioxidant, anti-inflammatory, and antibacterial properties that contribute to the observed wound healing properties. The phytoconstituents were sequentially extracted from the powdered leaves of *C. odorata* (L.) and chemoprofiled using the LC-MS technique. Furthermore, copper oxide/copper nanoparticles (CuNPs) were synthesized by the use of water extracts from the leaves of *C. odorata* (L.), characterized and evaluated for their potential biological and wound healing impacts. In this relation, scutellarein, isosakuranetin, and rutin, along with 15 other phytoconstituents were identified. Higher antioxidant (79.2% at 200 µg/mL) and anti-inflammatory potentials (66.8%) were obtained for CuNPs (120 µg/mL), in the size range of  $66.8 \pm 24.8$  nm. Antibacterial activity against methicillin-resistant *Staphylococcus aureus* and *Pseudomonas sp.* demonstrated mean zones of inhibition of  $16.7 \pm 4$  mm and  $17.73 \pm 2$  mm, respectively. Hence, the synthesized CuNPs would be desirable for inclusion in nanofibrous medical dressings.

### ARTICLE HISTORY

Received: 02 July 2023

Revised: 04 September 2023

Accepted: 09 September 2023

ePublished: 26 September 2023

### KEYWORDS

Biological functions  
*Chromolaena odorata* (L.) (Siam weed)  
 Copper oxide/copper nanoparticles (CuNPs)  
 Leaf extracts  
 Phytoconstituents  
 Wound healing potential

doi: [10.30495/tpr.2023.1990359.1363](https://doi.org/10.30495/tpr.2023.1990359.1363)

### 1. Introduction

Phytochemicals, often described as secondary metabolites of plants, possess a gamut of biological functions such as antioxidant, anti-inflammatory, and antimicrobial functions, as well as specialized protective abilities for cardiac, neuro, nephro, and gastrointestinal cells. Polyphenols are well-known antioxidants and include two important classes, namely flavonoids and phenolic acids, which are recognized globally in traditional medicine for their beneficial biological functions (Panche et al., 2016; Tungmunnithum et al., 2018). Approximately, 25% of available drugs/medicines are derived from the constituents of medicinal plants (Vitalini et al., 2009) and described either as infusions or decoctions. From ethnobotanical investigations including 66 species from 35 families, approximately 51.5% of the plant species were used to treat different ailments of

the gastrointestinal tract in humans, while 56% of the plants were used in cookery, 24.2% in veterinary, and 3.0% as cosmetics (Vitalini et al., 2013). The priority plant parts in the preparation of traditional medicine are leaves (37%) followed by whole plant (12.3%), fruits (11.1%), bark (8.6%), roots and bulbs (7%) and seeds (4.9%) (Guler et al., 2021). The anatomy and morphology of the stems and leaves of three *Salvia* spp. (L.), an endemic medicinal plant, were characterized by scanning electron microscopy and identified subtle differences between the species that are of significance in ethnopharmacological mapping in different ecosystems (Polat et al., 2017). Amirahmadi et al. (2022) studied the diversity of medicinal plants present in the province of Semnan, which will aid in the search for therapeutic agents that can benefit human beings. A variety of compounds extracted from different parts of plants, viz. leaf extracts of *Calendula officinalis* (L.) & *Rumex acetosa* (L.), and seeds of *Plantago ovata* Forsk

✉ Corresponding author: Sobha Kota

Tel: 0863-2232505; Fax: 0863-2350343

E-mail address: [sobhakota2005@gmail.com](mailto:sobhakota2005@gmail.com), doi: [10.30495/tpr.2023.1990359.1363](https://doi.org/10.30495/tpr.2023.1990359.1363)

have been used for the synthesis of silver/silver chloride nanoparticles, nickel, and magnetized nanospheres, respectively (Kota et al., 2017; Zhang et al., 2021; Mahdavi et al., 2022).

Herbs from the Asteraceae family are rich sources of bioactive compounds, e.g., 1,8-cineole,  $\alpha$ -pinene,  $\beta$ -pinene, camphor, sabinene, and kaempferol that can be used as natural and safe medicines for the treatment of a variety of illnesses/disorders (Kazeminia et al., 2022). *Chromolaena odorata* (L.) identified by R. M. King and H. Rob is one such perennial of the family Asteraceae with a broad distribution in the neotropical region of the world. *C. odorata* (L.) occupies 14.3% (7,892,447 km<sup>2</sup>) of the global land surface and is widespread in all continents except Antarctica. The distribution of *C. odorata* (L.) is 76.2% in South America, followed by 30.5% in Africa, 21.8% in Australia, 20% in Oceania, 13.2% in Asia, 6.4% in North America, and only 0.4% in Europe (Adhikari et al., 2023). The leaves of the plant are reported to possess medicinal value and are part of folk or traditional medicine in different parts of the world, particularly in Nigeria and Vietnam, which are African and Asian countries, respectively. The juice obtained from the plant is used as a hemostatic agent to stop bleeding from cuts and the nose (Phan et al., 2001). The aqueous leaf extract is used as an antiseptic agent in wound dressings, and the decoction is used for treating different diseases, namely diarrhea, malarial fever, diabetes, toothache, skin diseases, dysentery, and colitis (Akinmoladun and Akinloye, 2007). The medicinal value is assigned to the existence of various phytochemicals, such as alkaloids, tannins, flavonoids, and other phenolic compounds (Phan et al., 2001). The rich phytochemical composition of the plant endows it with anticancer, antihepatotoxic, anti-inflammatory, antimicrobial, and antioxidant functions (Sirinthipaporn and Jiraungkoorskul, 2017). Early research reports demonstrated the hemostatic (Wongkrajang et al., 1994) and wound healing capacity (Phan et al., 1998) of the *C. odorata* (L.) extract, but neither the mechanism nor the specific compounds involved in wound healing process were identified. Disruptions in the normal wound healing mechanism result in chronic wounds that are frequently accompanied by infections and sepsis. Hemostasis, inflammation, proliferation, and remodeling are the steps that are effectively completed within 4 to 6 weeks of an effective therapy (Moroz and Deffune, 2013; Morey et al., 2019; Akrawi et al., 2020). Scientific reports have revealed that phenolic compounds protect skin cell cultures from oxidative damage and promote tissue repair and represent wound healing signs (Phan et al., 2001; Thang et al., 2001). Recent studies have demonstrated that silver-silver chloride (Ag@AgCl) (Nguyen et al., 2020), magnesium oxide (Essien et al., 2020), silver (Jagatheesh et al., 2020), and silver-zerovalent iron nanoparticles (Jayeoye et al., 2021) can be synthesized from *C. odorata* (L.) leaf extract and established their antioxidant, antimicrobial, and anti-inflammatory activities, which together affect a faster wound healing process. Research studies reveal that medicinal plants are efficient in treating livestock

diseases that predominantly include gastrointestinal disturbances, foot and mouth disease, wounds and fractures, etc. in goats, cows, horses, sheep, cats, dogs, and other animals causing morbidity and mortality (Guler et al., 2021). One of the current challenges in medicine is the availability of effective treatment strategies associated with wounds of different types which are in some cases challenged with additional burdens such as diabetes, infections and others. Plant materials and their infusions/decoctions have been extensively used since ancient times, but the use of traditional knowledge is currently declining with the advent of synthetic drugs/medicines, which have the advantages of quick relief, and ease of manufacture. However, these drugs are associated with innumerable side effects including the serious problem of drug resistance.

With the aim of reintroducing our natural medicinal resources for potential benefits, the current study included the synthesis of copper nanoparticles (SWLE\_CuNPs) using the aqueous leaf extract of the widely distributed Siam weed for their possible use in wound dressings. The present study focuses on the phytochemical screening of *C. odorata* (L.) extracts and identification of the chemical moieties that contribute to the biological functions of wound healing through LC-MS profiling. The production of copper nanoparticles by the digestion method from the leaf extract of *C. odorata* (L.) using a stirred tank reactor is a new approach, and their measured antioxidant, anti-inflammatory, and antimicrobial activities are compared with those of the aqueous leaf extract of *C. odorata* (L.) and commercial CuO for the fabrication of phytoconstituent-enriched wound dressings.

## 2. Experimental

### 2.1. Acquisition of *C. odorata* (L.) plant leaves and Soxhlet extraction

Fresh leaves of *C. odorata* (L.) distributed in the Mahendragiri hills (Eastern Ghats: 18° 57' 59" N and 84° 21' 54" E), located at the border of Odisha and Andhra Pradesh, India, were procured and shade dried. The dry leaves were powdered using a mechanical blender. This leaf powder weighing 60 g (per batch) was sequentially subjected to the extraction using a Soxhlet apparatus with solvents of increasing polarity, i.e., hexane (1.0), ethyl acetate (0.228), acetone (0.355), and water (Raaman, 2006). The extracts were screened by standard tests to identify the phytoconstituents, i.e., alkaloids (Dragendorff's, Mayer's test), flavonoids (Alkaline reagent test, H<sub>2</sub>SO<sub>4</sub>, lead acetate test, Shinoda's test), sterols (Liebermann-Burchard's test), terpenoids (Liebermann test), anthraquinone (Borntrager's test), anthocyanin (HCl test), proteins (Biuret test, Ninhydrin test, Xanthoproteic test), phenolic compounds, quinones (Alcoholic KOH test, Conc. HCl test), and carbohydrates (Molish's test, Fehling's test) (Table S1). Furthermore, Soxhlet extraction of the leaf powder was performed individually with isopropanol and ethanol (70%) for a comparative analysis of the phytoconstituents, and the ethanol (70%) extract was subjected to LC-MS profiling.



## 2.2. Sample preparation and LC-MS analysis

*C. odorata* (L.) leaf powder (25 g) was first placed in 0.5 L of ethanol (70 v/v%), the obtained extract was then filtered using Whatmann's filter paper, condensed in a rotary vacuum evaporator at 40 °C, and the phenolic-rich orange-brown residue was stored at 20 °C until further use. The phytochemicals in the extract were evaluated using an Agilent 1290 Infinity II with a 6495 triple quad LC/MS unit equipped with an Agilent SB-C18 column. Furthermore, 45 mg of the phenolic-rich extract was solubilized in aqueous methanol (50 v/v%), centrifuged at 10 K rpm for 5 min, and the supernatant was used for LC-MS analysis (Eze and Tola, 2020).

## 2.3. Synthesis of copper nanoparticles in a stirred tank reactor

To 1 L of water, 60 g of *C. odorata* (L.) powder was added and kept at 80 °C for 1 h on a hot plate. The extract was then filtered to remove the leaf powder after cooling to room temperature, and the measured volume was approximately 700 mL every time. Copper sulfate solution was prepared by dissolving 1.4 g of copper sulfate pentahydrate ( $\text{CuSO}_4 \cdot 5\text{H}_2\text{O}$ ) in 20 mL of deionized (DI) water. The filtered aqueous extract and the copper sulfate solution were mixed in a volume ratio of 80:20 in a stirred tank reactor for 3 h at 60 °C. After the change in color to brown/black, the reactor was evacuated and the solution was centrifuged at 10 K rpm for 15 min. The nanoparticles formed were finally collected and kept in a hot air oven at 60 °C overnight for demoinsturation.

## 2.4. Characterization of the CuNPs

The synthesized CuNPs were analytically characterized using a combination of instrumentation involving UV-Vis spectrophotometry, field emission scanning electron microscopy (FESEM), Fourier transform infrared (FTIR) spectroscopy, X-ray diffraction (XRD), and thermogravimetric analysis (TGA) (Exstar/6300 thermogravimetric analyzer). The size, crystallinity, and morphology of the copper nanoparticles were deduced from XRD (Rigaku X-ray diffractometer Ultima IV 2036E202) and FESEM data (TESCAN-MIRA 3 XMU). The role of Siam weed leaf extract in the synthesis of copper nanoparticles and the functional groups available with the green synthesized SWLE\_CuNPs were confirmed using FTIR (Shimadzu, Miracle 10).

## 2.5. Antioxidant activities

All the experimental results obtained in triplicate were taken into consideration to measure the statistical parameters.

### 2.5.1. DPPH assay for free radical forage activity

The free radical scavenging/foraging activity of CuNPs was measured by the DPPH assay with a slightly modified protocol of Hsu et al. (2007). Accordingly, the experimental tubes were prepared with 2.5 mL of

DI water, 1.5 mL of DPPH (0.3 mM) in methanol, and specified concentrations of CuNPs (40, 80, 120, 160, and 200  $\mu\text{g}/\text{mL}$ ) were mixed and kept in an aphotic chamber at room temperature for 30 min. Simultaneously, a control containing 2.5 mL of DI water and 1.5 mL of DPPH (0.3 mM) was run in parallel with the experimental tubes. Different aliquots of ascorbic acid (40, 80, 120, 160, and 200  $\text{ng}/\text{mL}$ ) were used as positive controls. To each tube containing the ascorbic acid solution, 2.5 mL of deionized water and 1.5 mL of DPPH (0.3 mM) were added, and the reduction of DPPH was measured at 517 nm using a UV-Vis. spectrophotometer (Labindia, Model: UV3200). The percentage of antioxidant activity was determined as follows:

$$\text{Free radical scavenging in per cent of DPPH} = \frac{(\text{Ac} - \text{At})}{\text{Ac}} \times 100 \quad (\text{Eqn. 1})$$

Where Ac and At account for the absorbance of the control and the test/standard, respectively. The graph was plotted with the percent DPPH scavenging activity as a function of the concentration of CuNPs ( $\mu\text{g}/\text{mL}$ ). From the regression equation, the  $\text{IC}_{100}$  was calculated and ANOVA was performed.

### 2.5.2. $\text{KMnO}_4$ assay

The antioxidant activity of copper nanoparticles was determined using potassium permanganate ( $\text{KMnO}_4$ ) assay following the protocol reported by Amponsah et al. (2016). Briefly, phosphate buffer solution at pH 9 was prepared by dissolving 8.7 g of  $\text{KH}_2\text{PO}_4$  in 400 mL of DI water. A small quantity of  $\text{KMnO}_4$  (80 mg) was added and dissolved in 1 L of this phosphate buffer. The reaction mixtures were prepared by mixing 3 mL of  $\text{KMnO}_4$  with different concentrations of CuNPs, viz., 40, 80, 120, 160, and 200  $\mu\text{g}/\text{mL}$  and incubating in the dark for 30 min at room temperature. A solution containing 1 mL of DI water and 3 mL of  $\text{KMnO}_4$  was used as the control. Ascorbic acid at the same concentrations as the test (40, 80, 120, 160, and 200  $\mu\text{g}/\text{mL}$ ) served as the standard. Optical density (OD) was measured at 525 nm against the phosphate buffer.

### 2.5.3. ABTS assay for radical scavenge/forage ability

The ABTS assay described by Adedapo et al. (2009) was performed to estimate the free radical forage ability of the copper nanoparticles. Equivalent volumes of ABTS (7 mM) and potassium persulfate (2.4 mM) stock solutions were mixed and kept overnight at ambient temperature in an aphotic chamber until use. The working standard was prepared by adding 1 mL of stock solution to 60 mL of methanol, and an absorbance of  $0.7 \pm 0.001$  units was measured at 734 nm using a spectrophotometer. To the chosen concentrations of copper nanoparticles (40, 80, 120, 160, 200  $\mu\text{g}/\text{mL}$ ) and standard ascorbic acid (40, 80, 120, 160, 200  $\mu\text{g}/\text{mL}$ ), 3 mL of ABTS solution and 1 mL of DI water were added and kept at room temperature for 20 min. A control reaction tube was placed under the same conditions with 3 mL of ABTS and 1 mL of water. After incubation, the ABTS radical forage ability was calculated using the following equation:

$$\% \text{ Inhibition} = \frac{[(\text{Abs of control} - \text{Abs of sample})]}{(\text{Abs of control})} \times 100 \quad (\text{Eqn. 2})$$

here 'Abs' denotes absorbance.

## 2.6. *In vitro* anti-inflammatory activity

### 2.6.1. Membrane protection

Human red blood cell membrane stabilization was used to test the anti-inflammatory activity of copper nanoparticles *in vitro* (Vane and Botting, 1995). With informed consent, 2 mL of blood was drawn in a heparinized, purple-capped ethylene diamine tetraacetic acid (EDTA) tube from healthy volunteers who had not received any medication for at least two weeks. To separate the RBC and plasma, the test sample was centrifuged at 3000 revolutions per min for 15 min, and the obtained RBC was washed several times with isosaline (0.9% NaCl) and centrifuged. A 10% v/v solution was prepared by diluting the centrifuged solution with isosaline.

### 2.6.2. Hypotonicity induced hemolysis

To various concentrations of copper nanoparticles (0-120 µg/mL), 0.5 mL of HRBC suspension, 2 mL of hyposaline (0.2%), and 1 mL of phosphate buffer (0.15 mM) at pH 7.4 were added. For control, demineralized (DM) water was added instead of hyposaline. Diclofenac was used as the standard reference. The analysis tubes were maintained at 37 °C for 30 min and centrifuged at 3000 rpm for 15 min. The supernatant was analyzed spectrophotometrically at 560 nm to determine the percentage of hemoglobin. The percentage of hemolysis was calculated using the following formula:

$$\text{Hemolysis\%} = (\text{Absorbance of sample} / \text{Absorbance of control}) \times 100 \quad (\text{Eqn. 3})$$

$$\text{Percentage of protection} = 100 - \text{hemolysis in percentage} \quad (\text{Eqn. 4})$$

## 2.7. Antibacterial assay

The antibacterial capacity of the SWLE\_CuNPs and solvent (water) extracts of the leaves of Siam weed were tested against two pathogenic human clinical isolates, *e.g.*, methicillin-resistant *Staphylococcus aureus* (MRSA) and *Pseudomonas sp.* from three different patients, procured from the stock collection of the Department of Microbiology Culture Center of the local multispeciality hospital and medical college, as per the institutional ethical committee guidelines. The agar well diffusion method was used to evaluate the antibacterial potential. Clinical isolates were cultured in peptone water medium under aerobic conditions at 37 °C for 24 h. After two passes, the bacterial cells were grown in the nutrient broth (Hi-Media), harvested at an optical density (OD) of 0.6 and used for antibacterial activity evaluation. We used resazurin sodium extrapure dye to identify bacterial growth in the culture plates. While the actual color of the resazurin dye is purple, upon the growth of bacteria in the medium, the dye changes into a pink. Resazurin solution was prepared by adding 7.0 mg resazurin to 250 mL of DI water. To 90 mL of peptone-agar medium, 10 mL of resazurin dye solution was added just before pouring into petri plates and left

for solidification. With the help of a sterile cork borer, six wells of 6 mm depth were punched. 10, 25, 50, 75, and 100 µL of SWLE\_CuNPs in 5.0% dimethyl sulfoxide (DMSO) (50 mg/mL) were then taken and added in a clockwise direction in the order of wells labeled from 1 to 5. To the 6<sup>th</sup> well, 50 µL of 5.0% DMSO was added as a negative control. A 75/10 mcg ticarcillin/clavulanic acid (TCC) antibiotic disk was placed in the center of the Petri plate. The Petri plates were kept in a biochemical oxygen demand (BOD) incubator at 37 °C overnight. Zones of inhibition (ZOI) were measured using the Hi-Media scale.

## 3. Results and Discussion

### 3.1. Phytochemical analysis

Phytochemical tests were performed for the qualitative detection of bioactive chemical moieties in the prepared extract using an appropriate test method. Practically, every solvent has the capacity to dissolve specific solutes based on their polarity. A negative phytochemical test result should not be considered as the absence of a compound; *i.e.*, glycosides not detected in the qualitative test of the sample material extract were identified in LC-MS analysis. The LC-MS chemo-profile showed glycosidic compounds such as patulein 3-rhamnoside-7-(3,4-diacetylramnoside) and dihydroferulic acid 4-O-glucuronide. The phytochemical screening results of *C. odorata* (L.) with different solvents, namely hexane (non-polar), ethyl acetate (semi-polar), acetone (semi-polar), ethanol (polar), and water (polar) showed varying amounts of compounds, as expected. Leaf powder weighing 60 g was packed and subjected to Soxhlet extraction with 300 mL of each solvent and subsequently dried in a rotary vacuum evaporator. The quantity of semi-solid residue obtained was 352 mg with hexane, 533 mg with ethyl acetate, 0.8 mg with isopropanol, 1.1 g with acetone, 1.3 g with ethanol, and 1.6 g with water.

Interestingly, water contained the most number of compounds in the highest concentrations, as shown in Table 1. The hexane extract showed the presence of sterols, carbohydrates, and volatile oils. Flavonoids, sterols, carbohydrates, and proteins were present in the isopropanol, ethanol, and water extracts of *C. odorata* (L.), in alignment with the findings of a recently published report (Munira et al., 2022). Our earlier studies on the aqueous extracts of *Amaranthus viridis* (L.), *Hibiscus cannabinus* (L.), *Spinacea oleracea* (L.), *Mentha spicata* (L.), and *Coriandrum sativum* (L.) showed the presence of flavonoids, saponins, and tannins. *Alternanthera sessilis* (L.) is abundant in beneficial constituents such as flavonoids, terpenoids, phenols, phytosterols, and alkaloids (Kota et al., 2017, 2018). Isopropanol and ethanol extracts indicated positive tests for alkaloids and tannins in the phytochemical screening, and the same was confirmed from the LC-MS analysis with the presence of usnic acid (alkaloid) and quinic and gallic acids, which are classified as tannins, a class of complex phenolic compounds. Research findings revealed that the aerial parts of *Centaurea sps.* are rich in polyunsaturated fatty acids (approximately

**Table 1**

Phytochemical screening of *C. odorata* leaf extracts with various solvents in the order of increasing polarity.

Sr. No.	Phytoconstituent	Tests	H	EA	A	IP	E	DW
1	Alkaloids	Mayer's test	-	-	-	+	+	-
		Dragendorff's test	-	-	-	+	-	-
2	Flavonoids	Alkaline test	-	-	-	-	-	-
		Conc. H <sub>2</sub> SO <sub>4</sub>	-	-	-	+	+	+
		Lead acetate test	-	-	-	+	+	+
		Shinoda's test	-	-	-	-	-	-
3	Sterols	Libermann-Burchard's test	+	+	+	+	+	+
4	Terpenoids	Libermann test	-	-	-	-	-	-
5	Anthraquinone	Borntrager's test	-	-	+	+	+	-
6	Anthocyanin	HCl test	-	-	-	-	-	-
7	Proteins	Ninhydrin test	-	-	-	-	-	-
		Biuret test	-	-	-	-	-	-
		Xanthoproteic test	+	+	+	+	+	+
8	Phenolic compounds	Ferric chloride test	-	-	-	-	-	+
		Gelatin test	-	-	-	-	-	+
		Ellagic acid test	-	-	-	-	-	+
9	Quinones	Conc. HCl	-	-	-	+	-	-
		Alcoholic KOH	-	-	-	-	-	-
10	Carbohydrates	Molisch's test	+	+	+	+	+	+
		Fehling's test	+	+	+	+	+	+
11	Tannins	Braymer's test	-	-	-	+	+	-
		Gelatin test	-	-	-	+	+	-
		NaOH (10%) test	-	-	-	+	-	-
12	Saponins	Foam test	-	-	-	-	+	+
13	Cardiac glycosides	Baljet test	-	+	+	+	+	-
		Bromine water test	-	-	-	+	+	-
		Keller-killani test	-	+	+	+	+	-
14	Glycosides	Borntrager's test	-	-	-	-	-	-
		Aq. NaOH test	-	-	-	-	-	-
15	Lignin	Labat test	-	-	-	-	-	-
16	Coumarins	Fluorescence test	-	-	-	-	-	-
		NaOH test	-	-	-	-	-	-
17	Volatile oils	Fluorescence test	+	+	+	+	-	-

H: Hexane; EA: Ethyl acetate; A: Acetone; IP: Isopropanol; E: Ethanol; DW: Distilled water.

50% of the total fatty acids) and oleic acid, an essential monounsaturated fatty acid that could be used as a supplement to improve the health of humans (Erdogan et al., 2014). The phenolic acid compounds identified from the LC-MS chromatogram were quinic acid and gallic acid (Table 2). Quinic acid, a phenolic acid found in plants (Genc et al., 2022), is reported to regulate the fibronectin 1A (FN1A) and collagen 1A1 (COL1A1) genes that trigger their production. These molecules contribute significantly to the tissue repair process by affecting the migration and/or proliferation of fibroblasts (Genc et al., 2022), in addition to their antioxidant (preventing the formation of free radicals) and anti-inflammatory activities (NF-B inhibition) (Bhavna et al., 2017).

Gallic acid is a trihydroxybenzoic acid (phenolic acid) with remarkable antioxidant, antimicrobial, and anti-inflammatory properties. Two polyphenolic antioxidants, viz. lecanoric acid (which is also a dipeptide with two or more monocyclic aromatic units linked by an ester bond) and chlorogenic acid, were identified in the extract tested (Table 2) (Luo et al., 2009). Chlorogenic acid improves cellular proliferation and epithelialization (essential components of wound healing) and decreases nitric oxide and malondialdehyde, while increasing the reduced glutathione content. It suppresses IL-1, TNF-alpha, and IL-6 by inhibiting NF (Bagdas et al., 2015).

**Table 2**

 Compounds identified in *C. odorata* leaf extracts profiled by triple quad LC/MS analysis.

Sr. No.	Compound name	Predicted Formula	Retention time (min)	Mass	Height
45 mg of the phenolic-rich extract of <i>C. odorata</i> (L.) was solubilized in 50% aqueous methanol					
1	Quinic acid	C <sub>7</sub> H <sub>12</sub> O <sub>6</sub>	5.815	191	1.6×10 <sup>7</sup>
2	10-Hydroxymorrisonide	C <sub>17</sub> H <sub>26</sub> O <sub>12</sub>	28.136	481	1.27×10 <sup>7</sup>
3	Gallic acid	C <sub>7</sub> H <sub>6</sub> O <sub>5</sub>	7.456	125	6.12×10 <sup>6</sup>
4	Phenyl glucuronide	C <sub>12</sub> H <sub>14</sub> O <sub>7</sub>	34.423	315.1	1.49×10 <sup>7</sup>
5	Chlorogenic acid	C <sub>16</sub> H <sub>18</sub> O <sub>9</sub>	20.783	353.1	8.2×10 <sup>6</sup>
6	Uralennoiside	C <sub>12</sub> H <sub>14</sub> O <sub>8</sub>	42.386	285	1.18×10 <sup>7</sup>
7	Patulein 3-rhamnoside-7-(3,4-diacetylramnoside)	C <sub>32</sub> H <sub>36</sub> O <sub>18</sub>	21.191	707.1	2.2×10 <sup>6</sup>
8	2-HydroxybenzaldehydeO[xyllosyl-glucoside]	C <sub>18</sub> H <sub>24</sub> O <sub>11</sub>	22.724	415.1	0.95×10 <sup>7</sup>
9	Quercetin 3-O-(6-O-malonyl-β-D-glucoside)	C <sub>24</sub> H <sub>22</sub> O <sub>15</sub>	49.44	549	3.14×10 <sup>6</sup>
10	Dihydroferulic acid4-O-glucuronide	C <sub>16</sub> H <sub>20</sub> O <sub>10</sub>	24.172	371	6.4×10 <sup>6</sup>
11	Vitexin 4'-O-galactoside	C <sub>27</sub> H <sub>30</sub> O <sub>15</sub>	21.697	593.1	4.72×10 <sup>6</sup>
12	Rutin	C <sub>27</sub> H <sub>30</sub> O <sub>16</sub>	24.581	609.1	1.29×10 <sup>6</sup>
13	Apigenin 7-(2-acetyl-6-methylglucuronide)	C <sub>24</sub> H <sub>22</sub> O <sub>12</sub>	19.744	355	6.17×10 <sup>6</sup>
14	Lecanoric acid	C <sub>16</sub> H <sub>14</sub> O <sub>7</sub>	33.729	317	9.22×10 <sup>7</sup>
15	Hesperetin	C <sub>16</sub> H <sub>14</sub> O <sub>6</sub>	36.438	301	1.03×10 <sup>7</sup>
16	Trihydroxyoctadecenoic acid	C <sub>18</sub> H <sub>34</sub> O <sub>5</sub>	44.874	329.2	1.11×10 <sup>7</sup>
17	Luteolin	C <sub>15</sub> H <sub>10</sub> O <sub>6</sub>	42.386	285	1.17×10 <sup>7</sup>
18	Usnic acid	C <sub>18</sub> H <sub>16</sub> O <sub>7</sub>	40.383	343	0.87×10 <sup>7</sup>
Ethanollic (70%) extract					
1	Scutellarein	C <sub>15</sub> H <sub>10</sub> O <sub>6</sub>	8.325	285.2	8.325×10 <sup>6</sup>
2	Rutin	C <sub>27</sub> H <sub>30</sub> O <sub>16</sub>	13.837	609.5	3.5×10 <sup>6</sup>
3	Isosakuranetin	C <sub>16</sub> H <sub>14</sub> O <sub>5</sub>	8.201	284.4	5.3×10 <sup>6</sup>

Some flavonoids, such as quercetin 3-O-(6-O-malonyl-β-D-glucoside), rutin, apigenin 7-(2-acetyl-6-methylglucuronide), hesperetin, and luteolin (containing four hydroxyls) (Lo et al., 2021) have the desired antioxidant and/or anti-inflammatory potential (De Rango-Adem and Blay, 2021).

Rutin increases the production of antioxidant enzymes by inducing nuclear factor erythroid 2-related factor (NRF 2) and decreases the expression of matrix metalloproteinases and vascular endothelial growth factor. With these effects, rutin encourages wound healing and reduces the risk of ulcers (Chen et al., 2020). Morroniside, an iridoid glycoside, has antioxidant and antiapoptotic activity (Wang et al., 2008). According to Ma et al. (2022), morroniside reduces oxidative damage and apoptosis in ovarian granulosa cells induced by H<sub>2</sub>O<sub>2</sub>. Vitexin is an apigenin flavone glycoside with all three of the above-mentioned biological functions (Babaei et al., 2020). Usnic acid is a plant alkaloid with antimicrobial activity (Macedo et al., 2021). Phenyl glucuronide exhibits potent antioxidant activity. Along with the aforementioned compounds, the other

phytochemicals are phenyl glucuronide, uralennoiside, patulein 3-rhamnoside-7-(3,4-diacetylramnoside), 2-hydroxybenzaldehyde O-(xylosyl-glucoside), and trihydroxyoctadecenoic acid, all of which have essential biological functions in the human body (Table S2).

Chemo-profiling was performed using triple quad LC/MS to identify the phytoconstituents present in concentrated EtOH (70%) leaf extract (reduced to one-fifth of total volume using rotary vacuum evaporator), and the spectra revealed the presence of three bioactive compounds, namely rutin with a retention time (RT) of 13.3 min and an *m/z* ratio of 609.5, while scutellarein and/or isosakuranetin showed a RT of 8.3 min with an *m/z* ratio of 285.2. These results are in line with the earlier findings of Pandith et al. (2013), which revealed the occurrence of scutellarein, tetramethyl ether, isosakuranetin, and a stigmasterol in the ethanollic (70%) leaf extract of Siam weed leaves.

Lipopolysaccharide-induced inflammation increases the expression of the proinflammatory cytokines cyclooxygenase-2 (COX-2) and inducible nitric oxide synthase (iNOS), which in turn cause the release of prostaglandin E2 (PGE2) and nitric oxide (NO),

respectively. Suppression of NF- $\kappa$ B (p65) translocation into the nucleus through inhibition of I $\kappa$ B kinase complex alpha/beta (IKK alpha/beta) and inhibitory kappa-B-alpha (IKBalpha) by scutellarein (50  $\mu$ M), which further suppresses the expression of the COX-2 and iNOS enzymes, and consequent reduction in the release of PGE2 and NO, was first reported by Pandith et al. (2013). However, isosakuranetin, with its already established anti-inflammatory activity, did not demonstrate the suppression of either COX-2 or iNOS in this study; hence, it was inferred that its anti-inflammatory activity could be through a different mechanism independent of these two molecules.

Individual compounds in *C. odorata* (L.) extracts were identified by comparing MS data with European mass bank and relevant research data. The parameters that aid in the identification of bioactive compounds by chromatography are retention time, count (ion abundance) or relative intensity, and mass-to-charge ratio ( $m/z$ ). Table S2 lists the identified bioactive compounds, along with their IUPAC names, structures, and LC-MS peaks. Plant phenolics are specialized secondary metabolites associated with various health-promoting properties in humans. Flavonoids (quercetin 3-O-(6-O-malonyl- $\beta$ -D-glucoside), rutin, apigenin 7-(2-acetyl-6-methylglucuronide), hesperetin, luteolin, scutellarein, and isosakuranetin) (Table S2), glycosides (10-hydroxymorroniside, phenyl glucuronide, patulein 3-rhamnoside-7-(3,4-diacetyl)rhamnoside), dihydroferulic acid 4-O-glucuronide, and vitexin) (Table S3), phenolic compounds primarily in the form of phenolic acids (quinic acid, gallic acid) and polyphenols (lecanoric acid, chlorogenic acid) (Table S4), fatty acids (trihydroxyoctadecanoic acid) and alkaloids (usnic acid) (Table S5), and their derivatives that could serve as wellness-promoting bioactives, inferred from our obtained chromatogram, are presented in respective tables.

### 3.2. Synthesis and characterization of copper oxide/copper nanoparticles

The flavonoids found in the genus *Chromolaena* are considered valuable taxonomic markers (Eze and Jayeoye, 2021). Constrained by cost, availability, and other factors, we preferred to use aqueous extract for CuNP synthesis and aqueous leaf extracts for the evaluation of the relevant antimicrobial potential. For the manufacture of the wound dressing material, bulk production of copper nanoparticles using a simple protocol is warranted. Therefore, in the current study, a continuous stirred tank reactor of 5 L capacity with a total working volume of 2 L (aqueous leaf extract of *C. odorata* (L.) + copper sulfate solution) (vide materials and methods section) was run for 3 h at 60  $^{\circ}$ C. The average yield of the copper nanoparticles from the stirred tank reactor was 2.4 g/L of the processed volume (Weight of copper in 1.4 g copper sulfate pentahydrate is 0.35 g). The biosynthesized copper nanoparticles were characterized by UV-Vis spectrophotometry and showed maximum absorption at 440 nm (Fig. 1).

The absorption in the 400-440 nm range is due to

the charge transfer bands of O-Cu-O and Cu-O-CuO (Pestryakov et al., 2004). The size and surface morphology of the SWLE\_CuNPs as examined by FESEM indicate that the particles are within the nanoscale range of 35 to 100 nm and are spherical in nature (Fig. 2). While CuNPs synthesized from the extracts of leaves of *Aloe barbadensis* Miller (Liliaceae), the seeds of *Illicium verum* Hook. f. (Illiciaceae) & *Myristica fragrans* (Houtt.) (Myristicaceae), and the lacy covering of the seed (mace) of *M. fragrans* were in the size range of 80-120 nm, 210-270 nm, 170-210 nm, and 150-220 nm, respectively (Madiha et al., 2018; Vijayakumar et al., 2021), the CuNPs synthesized from *C. odorata* (L.) were very small, with a mean size of  $66.8 \pm 24.8$  nm. The commercial CuO nanoparticles were smaller with an average size of  $24.0 \pm 2.9$  nm, and spherical in shape (Fig. 3).

Energy dispersive spectroscopy (EDS) analysis of SWLE\_CuNPs revealed a peak for metallic copper, with the weight compositions for carbon, oxygen, and copper as 41.8%, 35.7%, and 15.2%, respectively. In addition, low-intensity peaks reflecting the presence of some elements, e.g., Na, P, S, and K in the spectrum confirm the capping of CuNPs with the organic phytoconstituents of *C. odorata* (L.) leaf extract (Fig. 4). The commercial CuO showed an intense peak for copper with a weight composition of 87.4%, and for oxygen, it was only 9.6% (Fig. 5).

The FTIR spectrum of commercial CuO showed absorption peaks at 432  $\text{cm}^{-1}$ , 447  $\text{cm}^{-1}$ , 486  $\text{cm}^{-1}$ , 540  $\text{cm}^{-1}$ , 594  $\text{cm}^{-1}$ , 648  $\text{cm}^{-1}$ , 686  $\text{cm}^{-1}$ , 725  $\text{cm}^{-1}$ , 871  $\text{cm}^{-1}$ , 910  $\text{cm}^{-1}$ , 1018  $\text{cm}^{-1}$ , 1357  $\text{cm}^{-1}$  and 1481  $\text{cm}^{-1}$  (Fig. S1a). The SWLE\_CuNP FTIR spectra showed absorption bands at 424  $\text{cm}^{-1}$ , 455  $\text{cm}^{-1}$ , 486  $\text{cm}^{-1}$ , 555  $\text{cm}^{-1}$ , 594  $\text{cm}^{-1}$  and these vibrations are attributed to the stretching vibrations of Cu(II)-O in CuO (Fig. S1b) (Mobarak et al., 2022; Tabrez et al., 2022). The spectral bands at 1587  $\text{cm}^{-1}$ , 1249  $\text{cm}^{-1}$  and 1064  $\text{cm}^{-1}$  correspond to the C-C stretching vibrations of aromatic compounds, C-O stretching of carboxylic acids, and ester bonds of phenolic compounds, respectively. The presence of all of these classes of organic compounds in the leaf extract of siam weed has been confirmed in our LC-MS analysis, and the same compounds were involved in the synthesis of copper nanoparticles (Kausar et al., 2022). The interaction between phytoconstituent functional groups and copper ions in  $\text{CuSO}_4$  resulted in the formation of copper nanoparticles. The green synthesis of copper nanoparticles from copper sulfate and plant extract occurs in three possible steps viz. copper ion production, reduction, and oxidation of reduced ions.

Match 2 software with the Crystallographic Open Database (COD) and Fullprof suite were used in the current analysis of XRD patterns for different phases. The corresponding entry numbers of COD/JCPDS are given in parentheses. The  $2\theta$  angles of  $32.4^{\circ}$  (110),  $35.6^{\circ}$  ( $-111$ ),  $38.6^{\circ}$  (111),  $48.7^{\circ}$  ( $-202$ ), and  $58.2^{\circ}$  (202) in the XRD pattern of native/amorphous SWLE\_CuNPs (Fig. 6a) matched with the monoclinic CuO tenorite (96-901-5823/01-089-2529) up to 96.6% and  $42.1^{\circ}$  (111),  $49.2^{\circ}$  (200),  $72.1^{\circ}$  (220) and  $87.3^{\circ}$  (311) matched with the cubic phase of Cu up to 3.4% (96-901-3024/04-

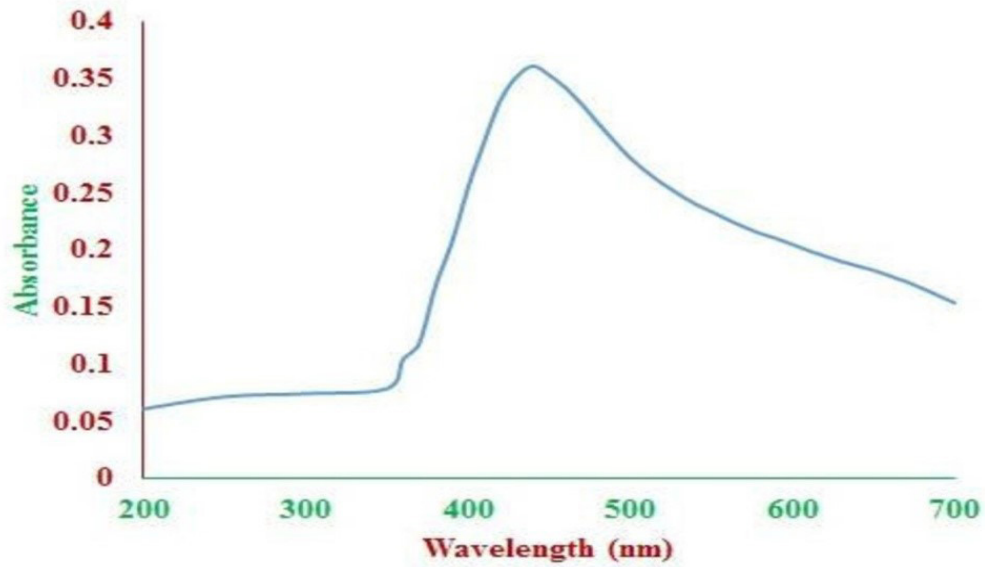


**Fig. 1.** UV-Vis spectrum of synthesized copper nanoparticles using *C. odorata* (L.) leaf extract.

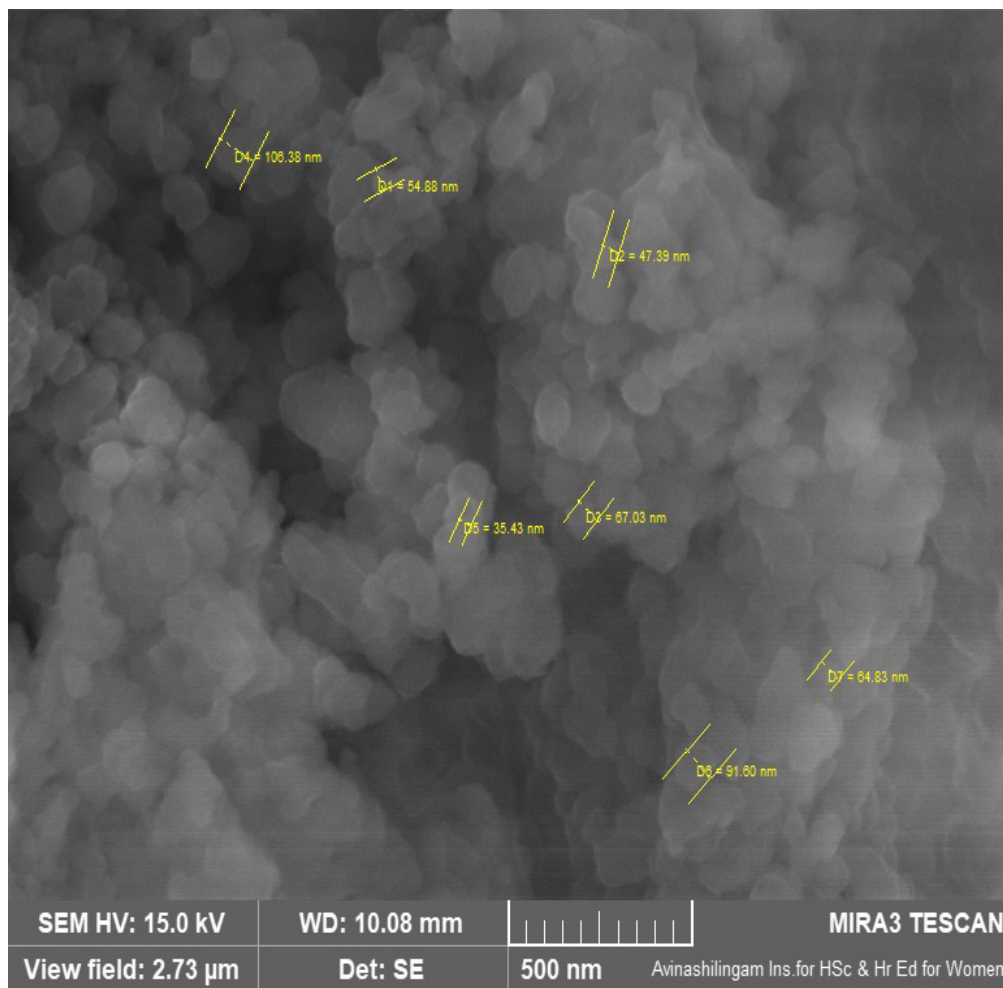


**Fig. 2.** FESEM pattern of copper nanoparticles (SWLE\_CuNPs) synthesized with aqueous leaf extract of *C. odorata*.

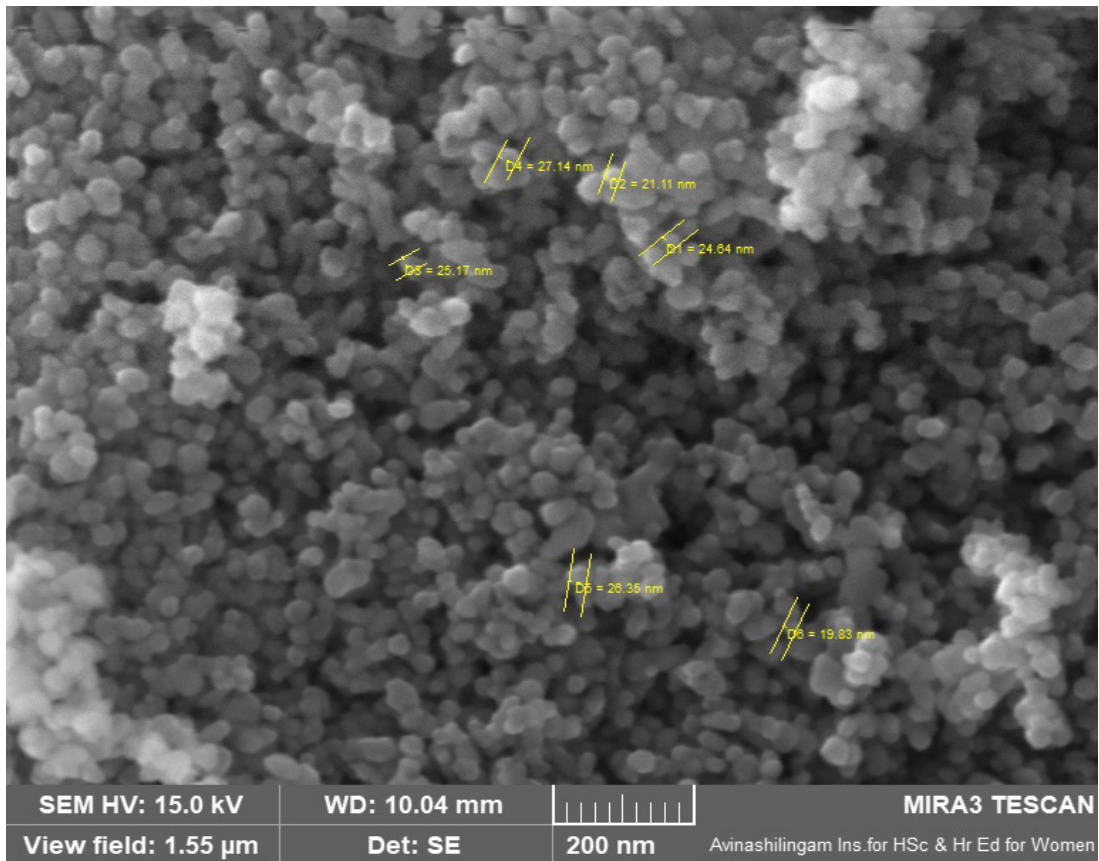


**Fig. 3.** FESEM pattern of commercial CuO nanoparticles.

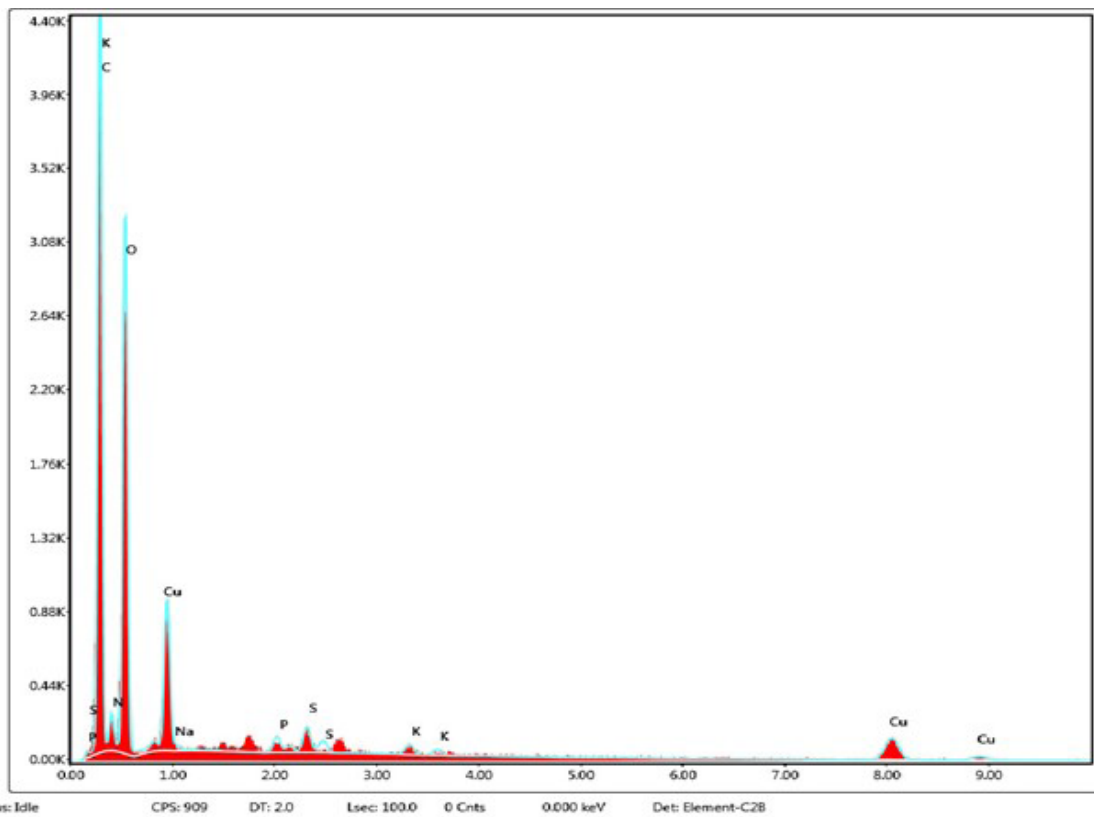


**Fig. 4.** Energy dispersive spectroscopic peaks denoting the presence of copper in SWLE\_CuNPs.

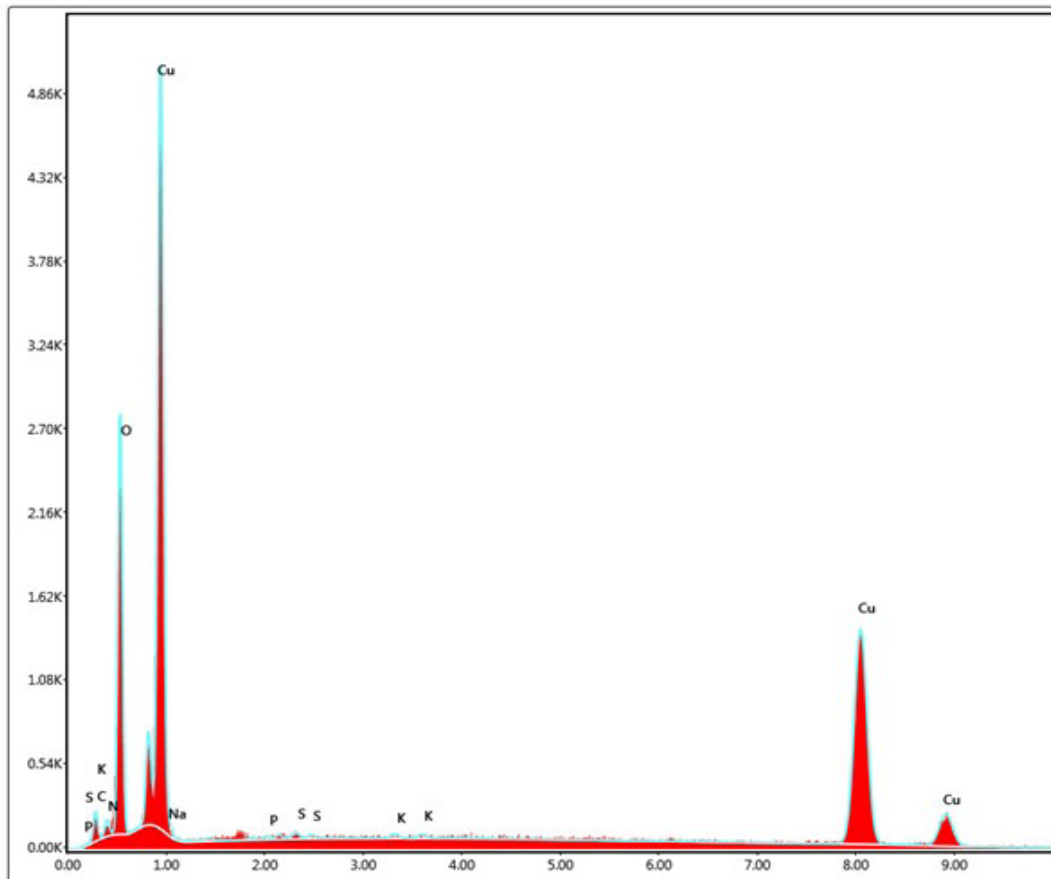


**Fig. 5.** Energy dispersive spectroscopic peaks indicating Cu in commercial CuO.

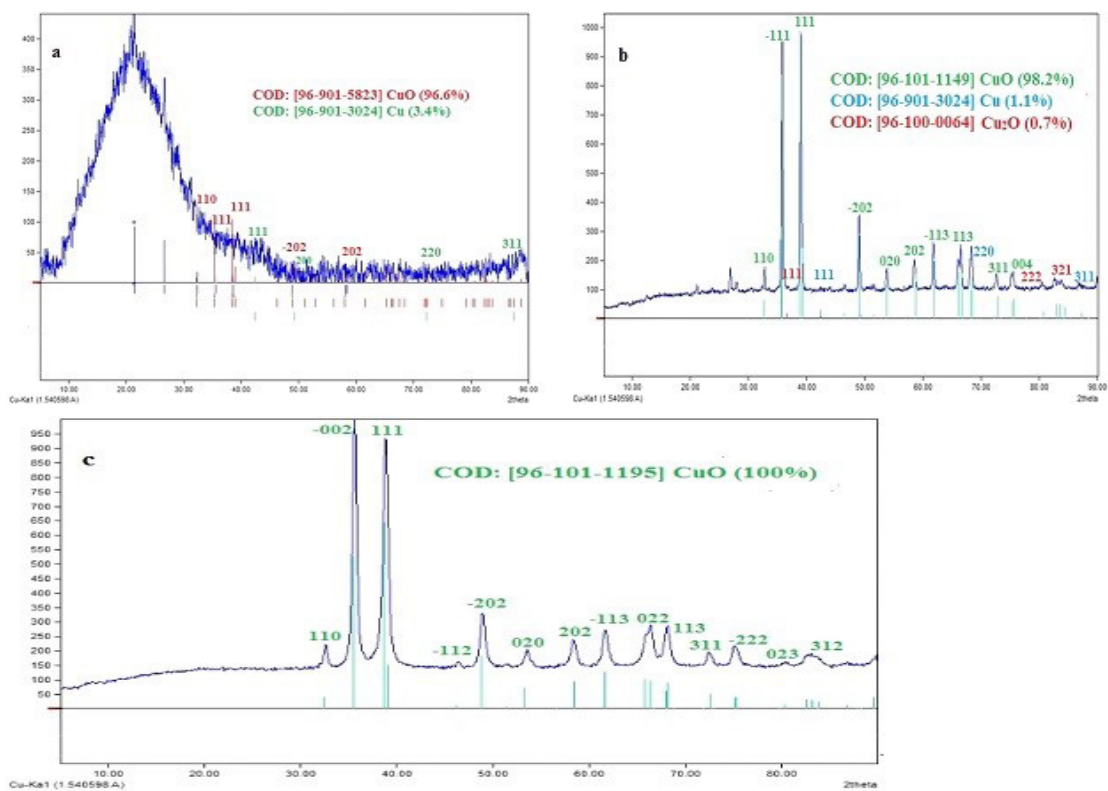


**Fig. 6.** XRD pattern of **a:** SWLE\_CuNPs (without annealing), **b:** SWLE\_CuNPs (after annealing) and **c:** Commercial CuO.

08366). Because the nanoparticles are capped with phytoconstituents, the intensities of the peaks are low. The XRD pattern of annealed SWLE\_CuNPs (Fig. 6b) showed peaks confirming the admixture of monoclinic tenorite phase of CuO (96.2%), cubic phase of Cu (1.1%) and cubic phase of Cu<sub>2</sub>O (0.7%). The peaks at 2θ angles of 32.8° (110), 35.8° (-111), 38.99° (111), 49.02° (-202), 53.73° (020), 61.8° (-113), 53.73° (020), 66.5° (-311), 68.3° (113), 72.9° (311), 75.4° (004) and 82.88° (-313) indicate the monoclinic tenorite phase of CuO (96-101-1149/01-089-2529).

The peaks at 2θ angles of 42.4° (111), 49.4° (200), 72.3° (220), and 87.6° (311) indicate the cubic phase of Cu (96-901-3024/04-08366), whereas the peaks at 2θ angles 36.6° (111), 69.9° (310), 73.8° (311), 77.7° (222), and 85.1° (321) indicate the cubic phase of Cu<sub>2</sub>O (96-100-0064/01-078-2076). The capping phytoconstituents are removed/decomposed during annealing, as evident from the intense, sharp peaks of the corresponding X-ray diffractogram. The mesospheric carbon-shelled copper nanoparticles showed peaks at 43.3° (111), 50.5° (200) and 74.1° (220), corresponding to the face-centred cubic nature (Huang et al., 2022). The peaks at 2θ positions 35°, 38°, 48°, 58°, 61°, 65°, 67° correspond to CuO; similar peaks at 26.7°, 38.8°, and 48.8° were reported for the green-synthesized CuONPs with *Propolis* extract (Hajizadeh et al., 2022); the peaks at 29°, 42°, 73° correspond to Cu<sub>2</sub>O (Fig. 6a); similar peaks at 29°, 36°, 42°, 61° and 73° were reported for the green-synthesized Cu<sub>2</sub>ONPs with *Phoenix dactylifera* L (Djamila et al., 2022), and the remaining peaks could be related to the presence of phytoconstituents. The XRD of commercial CuO denoted crystallinity of the sample with sharp peaks at 2θ positions 32.6° (110), 35.5° (002), 38.7° (111), 46.3° (-112), 48.8° (-202), 53.2° (020), 58.3° (202), 61.6° (-113), 65.7° (022), 68.1° (113), 71.8° (-312), 72.5° (311), 73° (221), 75.1° (-222), 80.4° (023) and 83.1° (312) (96-101-1195/01-089-2529) (Fig. 6c). The Scherer equation, used to calculate the particle size of the obtained SWLE\_CuNPs, is given below:

$$D = k\lambda/\beta\cos\theta \quad (\text{Eqn. 5})$$

Where D is the crystallite size, λ wavelength of the X-ray (wavelength of Cu Kα is 0.154 nm), β is the full width half maximum (0.6°), k is a constant (shape factor) 0.9, and θ is the diffraction angle (38.8°). The size of the SWLE\_CuNPs from the calculation deduced to be approximately 15.5 nm.

Thermogravimetric analysis confirmed the presence of phytoconstituents that function as reducing agents and form capping on the surface of SWLE\_CuNPs. The functional groups of flavonoids and the phenolic compounds (tautomeric transformation of enol to keto form releases hydrogen ions) sequentially reduce the copper sulfate into copper dihydroxide (Cu(OH)<sub>2</sub>), cuprous oxide (Cu<sub>2</sub>O), and on heating form into copper(Cu)/cupric oxide(CuO) nanoparticles (Gaba et al., 2022).



Derivative thermogravimetry (DTG) measures the rate at which the mass/weight changes as a function

of temperature. The DTG graph of SWLE\_CuNPs depicts varying rates of change of weight at different temperatures, viz. rate of change of weight at 75 °C was 60 µg/min; at 191 °C, it was 20 µg/min; at 262 °C reached a maximum of 160 µg/min, and then decreased steadily at a rate of 20 µg/min with the rise in temperature up to 950 °C (Fig. S2). From the differential thermal analysis (DTA) results, a small exothermic peak was identified at 834 °C. The total weight loss detected in the SWLE\_CuNPs' thermogravimetric analysis was 86.3% indicating that the green-synthesized copper nanoparticles with SWLE possessed a small percent of copper (13.7%) and were richly capped with the phytoconstituents (Fig. 7a). The organic phytoconstituents that coat the copper nanoparticles decompose in two stages or phases of temperature change: A 41.1% weight reduction at approximately 300 °C (first phase) and a 30.6% reduction at about 950 °C (second phase). The literature reports that copper nanoparticles synthesized with the extract of *Artemisia abyssinica* showed a decomposition peak at 284 °C which is quite close to our observations with SWLE (Achamo et al., 2022). From the DTG graph, the rate of change of weight for CuO (commercial) was slow from 100 °C to 780 °C and reached the maximum at 936 °C with 200 µg/min (Fig. S3). From the DTA analysis, an exothermic peak at 803 °C was noticed, which is in close alignment with our result. The total weight loss for the commercial sample of CuO as identified from the TG was 13.7%, and the remaining 86.3% was predominantly copper (Fig. 7b). Although the copper content in our prepared CuNPs is less, the biological functions of the NPs are significant because of the active phytoconstituents, and the use of such organically capped CuNPs is beneficial for the fabrication of the desired bioactive-enriched wound dressings.

### 3.3. Evaluation of biological functions

#### 3.3.1. Antioxidant activity

The antioxidant capacity of herbal plant extracts is often assigned to the presence of phenolic acids and flavonoids (Barmaverain et al., 2022). Copper nanoparticles' free radical scavenging activity, as measured by DPPH, KMnO<sub>4</sub>, and ABTS assays, is primarily determined by an antioxidant's ability to donate hydrogen ions, reducing free radical damage and promoting proper cellular function (Gudimella et al., 2022). Ascorbic acid is a well-known powerful antioxidant that has been used as the control for measuring free radical scavenging activity. The mean ± SD values of the DPPH assay of ascorbic acid (as standard), *C. odorata* (L.) leaf extract, SWLE\_CuNPs (green synthesized CuNPs), and commercial CuO are shown in Fig. 8a. The scavenging activity of ascorbic acid increased from 84.2 to 96.6%, a significantly higher value in comparison with the test samples (Fig. S4). The mechanism of scavenging free radicals is dependent on the ability of DPPH to accept hydrogen from ascorbic acid, *C. odorata* (L.) extract, SWLE\_CuNPs, and commercial CuO, to form a stable DPPH<sub>2</sub> complex. The percentage DPPH scavenging activity of SWLE\_CuNPs (11.2-43.9%), *C. odorata* (L.) extract (14.9-30.3%), and

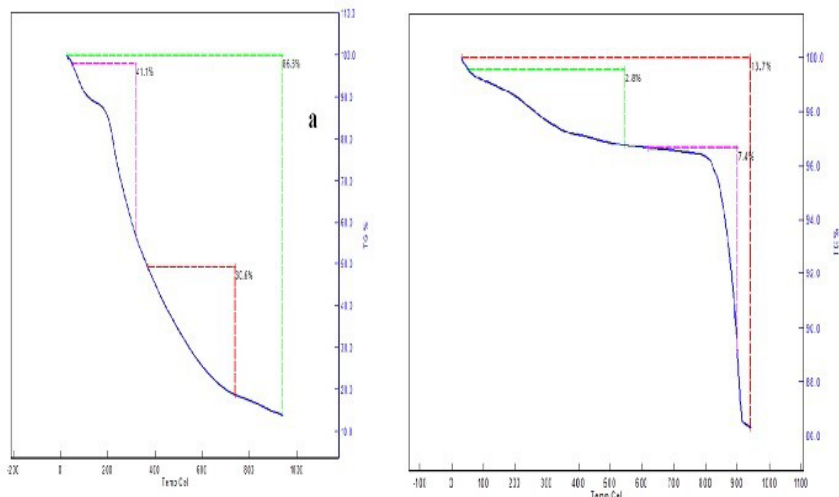


**Fig. 7.** Representation of the thermograms **a:** SWLE\_CuNPs and **b:** Commercially available CuO.

CuO(0.7-3.9%) (three test samples), as well as their corresponding linear regressions, are listed in Fig. 8a. The  $IC_{100}$  value for SWLE\_CuNPs, *C. odorata* (L.) leaf extract and commercial CuO obtained from the DPPH assay are 460.3  $\mu\text{g/mL}$ , 942.0  $\mu\text{g/mL}$  and 4880.3  $\mu\text{g/mL}$ , respectively. The lower  $IC_{100}$  values for commercial CuO are presumed to be due to the absence of organic coating by natural phytochemicals (Table 3). Ascorbic acid is a strong and potent antioxidant with very low  $IC_{100}$  value of 239.7  $\text{ng/mL}$  when compared to the test samples (SWLE\_CuNPs, *C. odorata* (L.) extract and CuO). As the direct intake of pure ascorbic acid is not advisable, the best alternative for fulfilling the human requirements are the natural and dietary plant antioxidants. Studies on antioxidant activity of various plant parts (roots, stem, leaves and tubers) of *Coleus forskohlii* (Willd.) Briq. indicate that tubers have the highest antioxidant activity followed by leaves, roots and stems, respectively (Khatun et al., 2011).

The antioxidant potential against  $\text{KMnO}_4$  reveals higher antioxidant activity by green synthesized CuNPs than the leaf extract alone, and commercial CuO. The antioxidant activity indicates the change in color from pink to yellow. Trends in the antioxidant activity of standard ascorbic acid (25.9 to 89.5%), SWLE\_CuNPs (19.8 to 57.2%), *C. odorata* (L.) extract (8.4 to 46.8%), and CuO (1.9 to 2.1%) are indicated in Fig. 8b, and Table 3 presents the linear regression equations as well as the  $R^2$  and  $IC_{100}$  values.

The ABTS radical scavenging activity is mainly due to the interaction between the antioxidant and the ABTS radical cation, which is indicated by a change in color from dark green to pale green. The radical scavenging activity of SWLE\_CuNPs increased from 28.2 to 79.2% with an increase in concentration from 40 to 200  $\mu\text{g/mL}$  (Fig. 8c), while the same for the standard ascorbic acid, *C. odorata* (L.) leaf extract, and commercial CuO were 69.3 to 89.9%, 26.3 to 47.4%, and 7.2 to 17.4%, respectively. Table 3 shows the linear regression

equations for the standard and test samples. In all the examined antioxidant assays of the three test samples, the SWLE\_CuNPs showed the highest scavenging activity due to the coating of nanoparticles with natural bioactive compounds present in *C. odorata* (L.) leaf extract. This is justified by the phenolics and flavonoids demonstrated from the phytochemical screening and LC-MS profiling.

### 3.3.2. In vitro anti-inflammatory activity

The anti-inflammatory drugs used to combat inflammation cause the stabilization of the lysosome membrane and prevent the release of acidic lysosomal enzymes into the cytosol. For experimentation, the RBC membrane stability is ideal and easy to investigate, and hence, the anti-inflammatory activity is tested with HRBC (Human Red Blood Corpuscles) by hypotonicity-induced hemolysis. Fig. 9 depicts the effect of SWLE\_CuNPs and standard diclofenac on HRBC membrane and the corresponding statistical data are presented in Table 3.

The reference diclofenac exhibited membrane protection to the extent of 71.5-92.3%, while the percentage of protection increased from 42.6 to 66.8% with the increase in concentration from 10 to 120  $\mu\text{g/mL}$  for SWLE\_CuNPs. This could be attributed to the inhibition of RBC membrane breakdown by the bioactive compounds and functional groups present on SWLE\_CuNPs. The  $IC_{100}$  value for diclofenac standard and SWLE\_CuNPs were 154.1  $\mu\text{g/mL}$  and 265.7  $\mu\text{g/mL}$  respectively. When RBC are treated with an isotonic solution of NaCl (0.9%), there are no alterations in the structure because of homeostasis (Fig. 10a). However, in a hypotonic solution (0.2% NaCl), more water enters the RBC resulting in rupture and the formation of "ghost cells" (Fig. 10b). The addition of SWLE\_CuNPs (10 mg CuNPs in 10 mL of hypo saline) stabilizes the membrane of the RBC due to the presence of anti-inflammatory

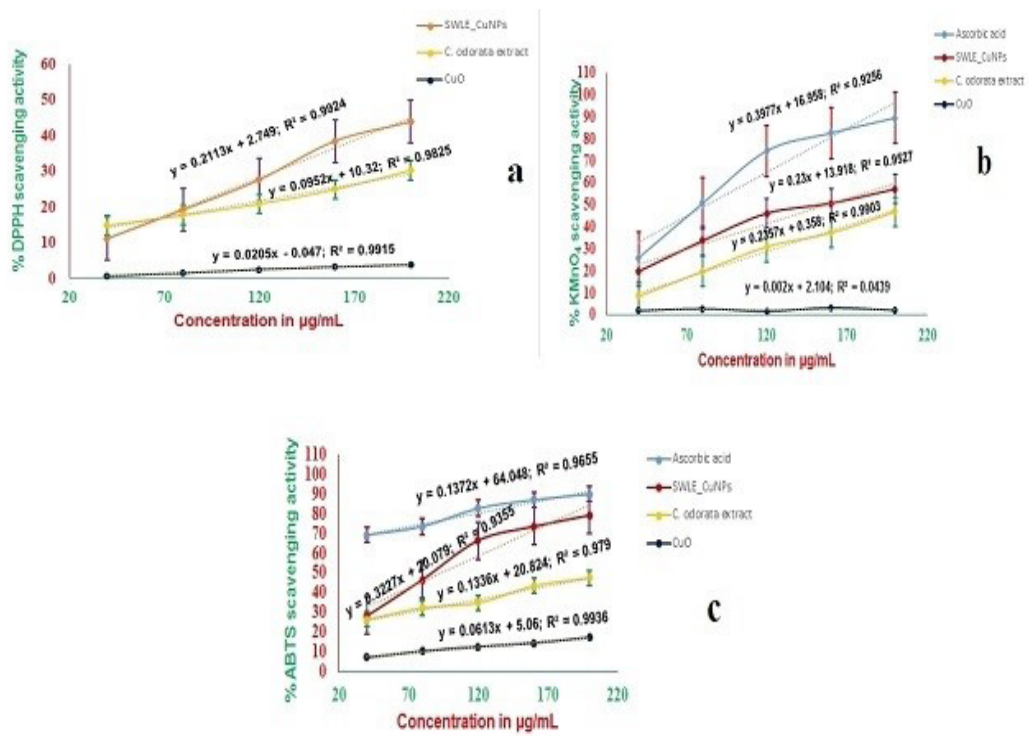


**Fig. 8. a:** DPPH scavenging activity, **b:** KMnO<sub>4</sub> Scavenging **c:** ABTS Scavenging of synthesized SWLE\_CuNPs, *C. odorata* leaf extract and commercial CuO.

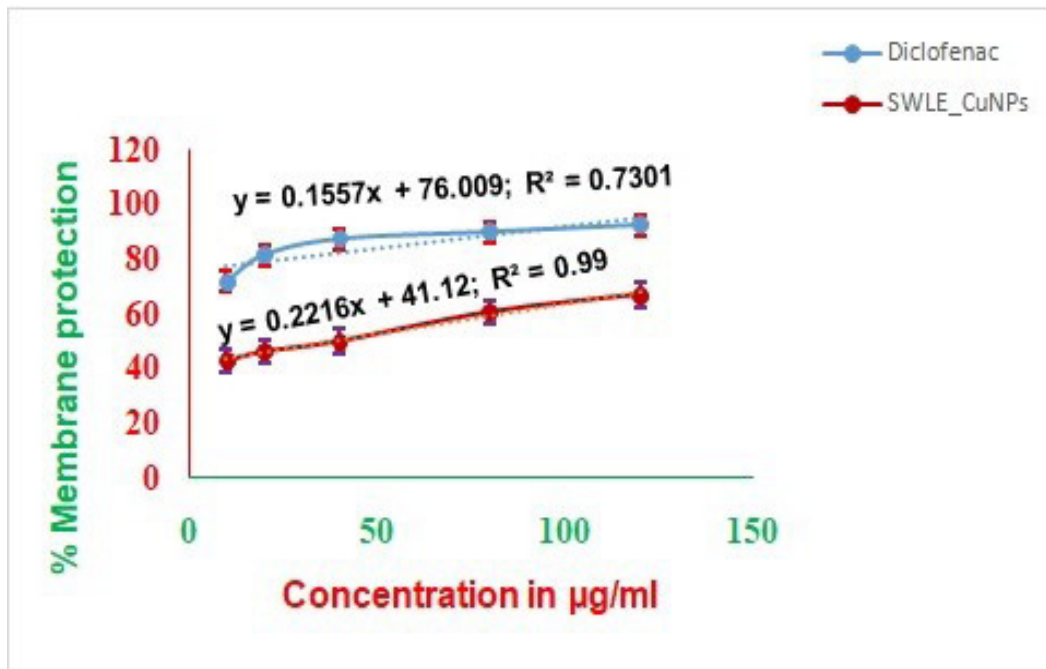


**Fig. 9.** Percentage of HRBC membrane protection by green synthesized SWLE\_CuNPs, in comparison with the standard anti-inflammatory drug, diclofenac.

**Table 3**

Results of one way analysis of variance (ANOVA) for the different antioxidant assays performed with the SWLE\_CuNPs, *C. odorata* leaf extract and commercial CuO.

Assay	Standard/test	IC <sub>100</sub> Concentration (µg/mL)	Results of One way Analysis of Variance (ANOVA)				
			Parameter	Sum of Squares (SS)	Degrees of Freedom (df)	Mean Square (MS)	F value
							p value with inference
DPPH	Ascorbic acid	239.7	Between groups	17880.3	3	5960.1	145.7
	SWLE_CuNPs	460.3	Within group	491	12	40.9	
	<i>C. odorata</i> (L.) extract	942	Total	18371.3	15	-	0.000 S
	Commercial CuO	4880.3					
KMnO <sub>4</sub>	Ascorbic acid	208.8	Between groups	10141.7	3	3380.6	12
	SWLE_CuNPs	374.3	Within group	4520.9	16	282.6	
	<i>C. odorata</i> (L.) extract	424	Total	14662.6	19	-	0.000 S
	Commercial CuO	48948					
ABTS	Ascorbic acid	262	Between groups	12807.1	3	4269	27.9
	SWLE_CuNPs	277.7	Within group	2445.2	16	152.8	
	<i>C. odorata</i> (L.) extract	592.6	Total	15252.4	19	-	0.000 S
	Commercial CuO	1548.8					
HRBC membrane stabilization	Diclofenac	154.1	Between groups	2454.2	1	2454.2	28.5
	SWLE_CuNPs	265.7	Within group	689	8	86.1	
			Total	3143.3	9	-	0.000 S

The *p* value is significant at  $p \leq 0.05$ ; S-Significant.

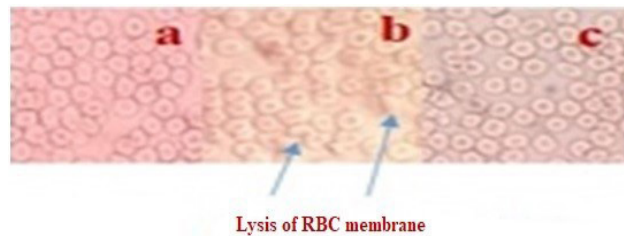


**Fig. 10.** a: RBC in isotonic solution b: Ruptured RBC in Hypotonic solution due to endosmosis c: Protection of RBC membrane by SWLE\_CuNPs.



phytoconstituents like scutellarein, quinic acid, rutin and others, as revealed by the LC-MS profile (Fig. 10c). Table 3 shows the results of ANOVA, a statistical analysis of antioxidant assays and anti-inflammatory activity. For all the tests, the  $p$  value was  $\leq 0.05$ , suggesting a significant difference between the groups in free-radical scavenging and membrane stabilization responses at different concentrations of test samples.

### 3.3.3. Antibacterial activity

Repeated administration of the antibiotics to inhibit the growth of these bacteria induces drug resistance in them over a period of time, and as a result, antibiotic-resistant strains dominate and wound healing turns into a challenge. If the subject is diabetic, then the control of infection becomes more challenging. To overcome these problems, one good choice evolved over the time is the utilization of metal nanoparticles like Ag and Cu, which are preferably green synthesized to ensure the availability of beneficial phytochemicals along with the antimicrobial metal nanoparticles. This methodology also delays drug resistance and reduces the dosage of antibiotic intake as the topical application of the wound dressings with these molecules will prevent infection, and even if the wound becomes infected, the bacterial load is kept below the thresholds, which otherwise causes severe stress. Gram-negative bacteria have thinner cell walls and are therefore more vulnerable to antibacterial agents.

Antimicrobial activity of SWLE\_CuNPs and *C. odorata* (L.) leaf extract and commercial CuO have been studied with two wound-specific bacterial strains, viz., methicillin-resistant *Staphylococcus aureus* (MRSA) and *Pseudomonas sp.*, from three different infected volunteers (Table 4, Table 5 and Table 6). From the results of the antibacterial assays conducted, the SWLE\_CuNPs were found effective against both the types of bacteria (independent of their cell wall composition), and the ZOI's spanned over  $\sim 9$  mm to  $\sim 15$  mm. Ticarcillin/clavulanate (TCC), an FDA (Food and drug administration) approved highly potent antibiotic is used clinically to treat a variety of bone and joint, skin and skin structure infections, but repeated use of this antibiotic induces drug resistance in bacteria. The rationale behind the use of this antibiotic specifically was to evaluate the efficacy of the SWLE and SWLE\_CuNPs against the methicillin resistant *S. aureus* and *Pseudomonas sp.* that are effectively inhibited by the combinational drug of TCC. Standard TCC, i.e., 75/10 mcg disks produced zones of inhibition against *Staphylococcus aureus* (ATCC 25923) and *Pseudomonas aeruginosa* (ATCC 27853) in the ranges of 29-37 mm and 20-28 mm respectively. The comparison of the antibacterial potential of SWLE\_CuNPs with the standard TCC revealed a significant gap in the efficiency between them. However, despite the relatively lower antibacterial potential of green-synthesized SWLE\_CuNPs, the latter may be preferred to prevent or minimize infections because of their multi-pronged biological protection in the healing process. The SWLE\_CuNPs revealed antibacterial activity, with the zones of inhibition (ZOI) ranging between 8.6 mm and 16.7 mm. MRSA isolate 1 showed a ZOI of  $15.3 \pm$

2.7 mm at 2.5 mg of the SWLE\_CuNPs, and with the increase in concentration of the SWLE\_CuNPs to 5 mg, the zone of inhibition marginally increased to  $16.7 \pm 3.9$  mm. For MRSA isolate 2, the increase in SWLE\_CuNPs concentration from 0.5 mg to 5 mg did not cause any significant difference in the ZOI. In the case of isolate 3, at 2.5 mg, the ZOI was  $14.1 \pm 3.1$  mm (Fig. 11a). Copper nanoparticles showed a maximum zone of inhibition of  $17.4 \pm 6.6$  mm against *Pseudomonas sp.* isolate 2, while with the increase in concentration of SWLE\_CuNPs from 1.25 mg to 3.75 mg, the increase in ZOI was negligible ( $15.3 \pm 8.7$  mm to  $16.8 \pm 8.1$  mm) (Fig. 11b). Siam weed leaf extract showed the highest ZOI of  $15 \pm 4.8$  mm at 3.75 mg against MRSA isolate 2 and the lowest ZOI of  $5.2 \pm 4.5$  mm at 1.25 mg (Fig. 11c and Fig. 11d). The proposed mechanism for the antimicrobial potential of the CuNPs is their adsorption ability to the cell membrane causing depolarization. Slavin et al. (2017) reported that the negative charge on the cell wall is changed by the CuNPs, and therefore the cell wall integrity is damaged. The other proposed mechanism suggests that the copper cations of nanoparticles interact with the cell wall lipids causing peroxidation and pore opening in cell membranes (Hong et al. 2012). Overall, the antimicrobial activity of SWLE\_CuNPs was greater than that of the extract alone against MRSA and *Pseudomonas sps* in all clinical isolates tested. The literature reports suggest that copper nanoparticles synthesized from the leaf extract of *Cordiamyxa L.* exhibited bacteriostatic activity against *Pseudomonas sps.* with an inhibition zone of 17.6 mm (Abbas et al., 2022). The green synthesized nano-sized cuprous oxide of *Allium cepa* and *Raphanus sativus* showed antibacterial activity with the ZOI of 16 mm and 18 mm respectively for *S. aureus* (Kumar and Reddy, 2022). These research results align with the findings of the current study in which the SWLE\_CuNPs showed average ZOI of  $17.7 \pm 1.9$  mm and  $16.7 \pm 3.9$  mm for the clinical isolates of *Pseudomonas sps.* and Methicillin resistant *Staphylococcus aureus* respectively. Smart-Dre-M: Biopolymer Composite-based Nano-Fibrous Wound Dressing Material, Indian Patent No. 202041052202; Published on 12.12.2020 (Smart-Dre-M, 2020) proposed natural and low-cost biomaterials for wound dressing that include a multi-layer electrospun core-shell nanofibrous scaffold. Wound dressings were fabricated using a chitosan-keratin-cellulose solution containing the leaf extract of *C. odorata* (L.) (Siam weed), which has hemostatic wound healing properties. In addition, the authors identified phytoconstituents found in native or local *C. odorata* (L.) leaves (Mahendragiri hills) as well as the interaction of their biological functions for effective wound healing. The findings of this study authenticate the presence of phytochemicals, viz., alkaloids, flavonoids, and sterols, which aid in wound healing. As a naturally bioactive component, *C. odorata* (L.) delays the onset of infection and alleviates antibiotic drug resistance. An efficient wound dressing prevents infection, restricts inflammation, promotes cell proliferation, and delivers drugs or bioactives to hasten healing. All these requirements for a wound dressing can be met by the use of *C. odorata* (L.) extract as one of the constituents in the dressing material.

**Table 4**

Results of one way analysis of variance (ANOVA) for the antibacterial activity of SWLE\_CuNPs.

Sr .No.	Sample tested	Name of the clinical pathogen	ZOI in mm expressed as Mean $\pm$ SD of triplicates							F value	
			Std. Ab	1	2	3	4	5	6	$p$ value with inference	
1	Isolate 1	Methicillin resistant <i>Staphylococcus aureus</i> (MRSA)	21.9 $\pm$ 2.2	8.6 $\pm$ 7.5**	13.6 $\pm$ 3.3	15.3 $\pm$ 2.7*	15.5 $\pm$ 1.8*	16.7 $\pm$ 3.9**	0 $\pm$ 0	4.4	0.01 S
			19.0 $\pm$ 6.4	14.5 $\pm$ 2.1	15.9 $\pm$ 4.0**	14.6 $\pm$ 3.1	15.8 $\pm$ 3.7**	14.0 $\pm$ 2.0	0 $\pm$ 0	0.6	0.7 NS
			27.7 $\pm$ 1.8	11 $\pm$ 9.5	12.8 $\pm$ 5.5	14.1 $\pm$ 3.4	14.5 $\pm$ 2.5	13.7 $\pm$ 2.4	0 $\pm$ 0	0.5	0.7 NS
1	Isolate 1	<i>Pseudomonas sp.</i>	29.2 $\pm$ 5.4	12.8 $\pm$ 4.6	15.2 $\pm$ 3.7**	16.3 $\pm$ 2.5	16.0 $\pm$ 1.0	15.1 $\pm$ 0.2**	0 $\pm$ 0	0.4	0.8 NS
			25.3 $\pm$ 2.3	12.1 $\pm$ 6.2	15.3 $\pm$ 8.7**	15.1 $\pm$ 10.0**	16.8 $\pm$ 8.1	17.4 $\pm$ 6.6	0 $\pm$ 0	0.5	0.7 NS
			22.8 $\pm$ 3.0	8.4 $\pm$ 1.0**	11 $\pm$ 2.7	12.0 $\pm$ 3.9**	14.4 $\pm$ 1.3**	17.4 $\pm$ 1.9**	0 $\pm$ 0	16.5	0 S

 Note: Ab: Antibiotic; The  $p$  value is significant at  $p < 0.05$ ; \*\*denotes  $p < 0.01$ ; \*denotes  $p < 0.05$ ; S-Significant; NS: Non-Significant.

**Table 5**

Results of one way analysis of variance (ANOVA) for the antibacterial activity of Siam weed extract.

Sr. No.	Sample tested	Name of the clinical pathogen	ZOI in mm expressed as Mean $\pm$ SD of triplicates							F value	
			Std. Ab	1	2	3	4	5	6	$p$ value with inference	
1	Isolate 1	Methicillin resistant <i>Staphylococcus aureus</i> (MRSA)	18.2 $\pm$ 4.9	0 $\pm$ 0**	7.7 $\pm$ 0.7**	9.1 $\pm$ 1.1**	7.1 $\pm$ 1.0**	7.5 $\pm$ 0.8**	0 $\pm$ 0	156.9	0 S
			20.2 $\pm$ 3.0	7.6 $\pm$ 7.3	14.1 $\pm$ 4.4	14.8 $\pm$ 4.6**	15 $\pm$ 4.8**	14.6 $\pm$ 5.0**	0 $\pm$ 0	2.8	0.05 NS
			25.7 $\pm$ 4.0	0 $\pm$ 0**	9.8 $\pm$ 1.2**	11.0 $\pm$ 2.4**	12.2 $\pm$ 0.2**	12.6 $\pm$ 0.6**	0 $\pm$ 0	144	0 S
1	Isolate 1	<i>Pseudomonas sp.</i>	26.2 $\pm$ 6.1	0 $\pm$ 0**	0 $\pm$ 0**	10.0 $\pm$ 4.7**	9.5 $\pm$ 2.0**	11.9 $\pm$ 3.0**	0 $\pm$ 0	38	0 S
			25.4 $\pm$ 1.4	8 $\pm$ 0.6	7.2 $\pm$ 0.6*	9.7 $\pm$ 3.6	14 $\pm$ 6.3*	10.6 $\pm$ 6.0	0 $\pm$ 0	3.2	0.04 S
			23.0 $\pm$ 6.2	5.3 $\pm$ 4.6**	5.2 $\pm$ 4.5**	8.6 $\pm$ 1.1	9.7 $\pm$ 2.0	10.7 $\pm$ 3.7*	0 $\pm$ 0	4.3	0.01 S

 Note: Ab: Antibiotic; The  $p$  value is significant at  $p < 0.05$ ; \*\*denotes  $p < 0.01$ ; \*denotes  $p < 0.05$ ; S-Significant; NS: Non-Significant.

**Table 6**

Results of one way analysis of variance (ANOVA) for the antibacterial activity of commercial CuO.

Sr .No.	Sample tested	Name of the clinical pathogen	ZOI in mm expressed as Mean $\pm$ SD of triplicates						F value	
			Std. Ab	1	2	3	4	5	6	$p$ value with inference
1	Isolate 1	Methicillin resistant <i>Staphylococcus aureus</i> (MRSA)	22.8 $\pm$ 8.9	0 $\pm$ 0	0 $\pm$ 0	0				
2	Isolate 2		21.2 $\pm$ 3.2	0 $\pm$ 0	0 $\pm$ 0	0				
3	Isolate 3		0 $\pm$ 0	0 $\pm$ 0	6.1 $\pm$ 5.6**	6.7 $\pm$ 6.6**	6.9 $\pm$ 6.3*	8 $\pm$ 7.0*	0 $\pm$ 0	5.9
1	Isolate 1	<i>Pseudomonas sp.</i>	31.7 $\pm$ 2.9	0 $\pm$ 0	0 $\pm$ 0	0				
2	Isolate 2		21.2 $\pm$ 3.2	6.9 $\pm$ 3.5**	6.8 $\pm$ 6.8**	7.9 $\pm$ 7.8**	9.4 $\pm$ 9.1**	11.1 $\pm$ 6.0**	0 $\pm$ 0	41.9
3	Isolate 3		24.6 $\pm$ 2.9	7.8 $\pm$ 3.9	7.7 $\pm$ 3.9	8.4 $\pm$ 4.2	8.9 $\pm$ 4.4	7.0 $\pm$ 3.5	0 $\pm$ 0	0.3
										0.9
										NS

Note: Ab: Antibiotic; The  $p$  value is significant at  $p < 0.05$ ; \*\*denotes  $p < 0.01$ ; \*denotes  $p < 0.05$ ; S-Significant; NS: Non-Significant.

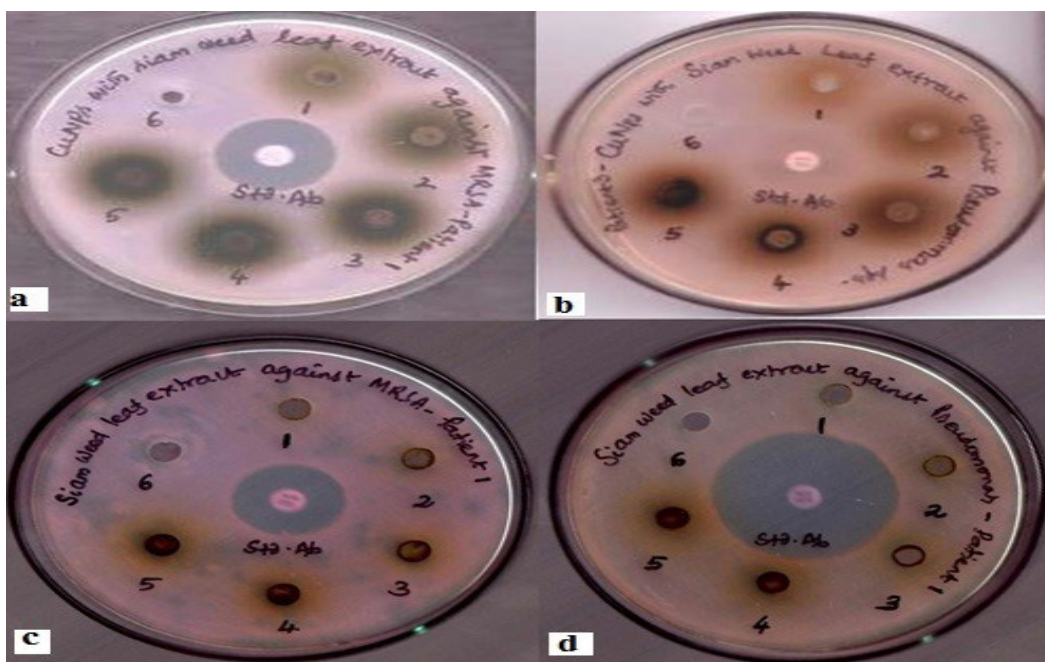


**Fig. 11.** Antibacterial activity of SWLE\_CuNPs against **a:** MRSA **b:** *Pseudomonas sp.*; Siam weed leaf extract against **c:** MRSA **d:** *Pseudomonas sp.*

#### 4. Concluding remarks

The findings of the current report revealed that the *C. odorata* (Siam weed) collected from the Mahendragiri Hills of the Eastern Ghats has excellent phytoconstituents, e.g., phenolic compounds, flavonoids, alkaloids, polyphenols, glycosides, and fatty acids, which can act as potential antioxidant, anti-inflammatory, and antimicrobial agents and capable of healing the wound. The LC-MS chemoprofile showed the presence of a number of potent natural compounds like scutellarein, isosakuranetin, quercetin 3-O-(6-O-malonyl-β-D-glucoside), and rutin that are found efficient in wound healing. SWLE\_CuNPs were characterized by FTIR, XRD, and TGA. The X-ray diffractogram of SWLE\_CuNPs shows the crystallinity of the material; the peaks (compared with JCPDS cards) denote the presence of three constituents, viz., Cu, CuO, and Cu<sub>2</sub>O. The TGA analysis clearly showed that the copper nanoparticles are coated by organic compounds (86.3%) that form the basis for the medicinal value of the leaves and the formation of CuNPs with the extract. The SWLE\_CuNPs exhibited more antioxidant, anti-inflammatory, and antimicrobial activity than the Siam weed extract and commercial CuO. Customized wound dressings to address the complex issues associated with different types of wounds, including traumatic, diabetic, infectious, and pressure ulcers, are the need of the hour. In this context, inspired by the current study results demonstrating extensive phytochemicals in *C. odorata* and its ability to form copper nanoparticles, it could be inferred that the plant bioactives-enriched nanofibrous wound dressings could be widely fabricated for use by clinicians and mitigate antibiotic-resistance-related complications in subjects with acute or chronic wounds.

#### Funding

This research was funded by the Department of Science and Technology-Advanced Manufacturing Technology Division, New Delhi, grant number "DST/TDT/AMT/2021/002".

#### Acknowledgements

KS and RS sincerely acknowledge the receipt of DST-AMT grant (No.: DST/TDT/AMT/2021/002) in support of the study. The authors place on record their sincere gratitude to the Department of Microbiology, Katuri Medical College, Guntur for supplying the clinical bacterial isolates. Also, authors gratefully acknowledge the support from Bharat Ratna Prof. C N Rao Research Center, Avinashilingam University, Coimbatore for utilization of characterization facility. Finally, authors owe their sincere thanks to the principal and the management of RVR & JC College of Engineering for the laboratory facilities and the encouragement.

#### Ethical guidelines

The experimental protocol for anti-inflammatory study involving human volunteers was strictly followed as

approved by the Institutional Ethical Committee (IEC/RVRJCCE/DST-AMT/2022-23/01).

#### Informed consent

Anti-inflammatory analysis of the blood samples was carried out with the informed consent of the volunteers (IEC/RVRJCCE/DST-AMT/2022-23/01).

#### Abbreviations

ABTS: 2,2'-Azino-bis(3-ethylbenzothiazoline-6-sulfonic acid); *C. odorata*: *Chromolaena odorata*; DPPH: 1,1-diphenyl-2-picrylhydrazyl; IL: Interleukin; MRSA: Methicillin-resistant *Staphylococcus aureus*; Std. Ab: Standard antibiotic; SWLE: Siam weed leaf extract; SWLE\_CuNPs: Siam weed leaf extract copper nanoparticles; TNF: Tumor necrosis factor.

#### Author contribution statement

Conceptualization, experimental design, analysis, characterization and interpretation of the obtained data were performed by Sobha Kota. Pradeep Dumpala prepared the manuscript and conducted the relevant experimental material collection along with the antibacterial activity evaluation. Radhika Sajja performed the statistical design of experiments and data analysis. Ratnakumari Anantha synthesized the copper nanoparticles, performed the corresponding antioxidant and anti-inflammatory activity evaluation and prepared the first draft of the manuscript. All authors read and approved the final manuscript.

#### Conflict of interest

The authors declare that there is no conflict of interest.

#### References

- Abbas, S.F., Ali, I.N., Kareem, S.H., Muhammed, S.A.E., 2022. Green Synthesis of Copper Nanoparticles From *Cordiamyxa* L. Leaves Ethanol Extract and Their Antibacterial Activity. AIP conference proceedings. 2386, 020028.
- Achamo, T., Zereffa, E.A., Ananda Murthy, H.C., Ramachandran, V.P., Balachandran, R., 2022. Phyto-mediated synthesis of copper oxide nanoparticles using *Artemisia abyssinica* leaf extract and its antioxidant, antimicrobial and DNA binding activities. Green Chem. Lett. Rev. 15(3), 598-614.
- Adedapo, A.A., Jimoh, F.O., Koduru, S., Masika, P.J., Afolayan, A.J., 2009. Assessment of the medicinal potentials of the methanol extracts of the leaves and stems of *Buddleja saligna*. BMC Complement Altern. Med. 9(1), 1-8.
- Adhikari, P., Lee, Y.-H., Poudel, A., Lee, G., Hong, S.-H., Park, Y.-S., 2023. Predicting the Impact of Climate change on the habitat distribution of *Parthenium hysterophorus* around the world and in South Korea. Biology 12(1), 84.
- Akinmoladun, A.C., Akinloye, O., 2007. Effect of *Chromolaena odorata* On Hypercholesterolemia Related



- Metabolic Imbalances. Proc. Akure-HumboldtKellog/3rd SAAT Annual Conference, FUTA, Nigeria, 287-290.
- Akrawi, S.H., Gorain, B., Nair, A.B., Choudhury, H., Pandey, M., Shah, J.N., Venugopal, K.N., 2020. Development and optimization of naringenin-loaded chitosan-coated nanoemulsion for topical therapy in wound healing. *Pharmaceutics* 12(9), 893.
- Amirahmadi A., Naderi, R., Afsharian, M.H., 2022. An investigation into the medicinal plants of Semnan province with taxonomic and therapeutic aspects. *Trends Phytochem. Res.* 6(4), 312-338.
- Amponsah, I.K., Orman, E., Mensah, A.Y., Sarpong, F.M., Armah, F.A., Sarpong, L.M., 2016. Development and validation of a radical scavenging antioxidant assay using potassium permanganate. *J. Sci. Innov. Res.* 5(2), 36-42.
- Babaei, F., Moafizad, A., Darvishvand, Z., Mirzababaei, M., Hosseinzadeh, H., Nassiri-Asl, M., 2020. Review of the effects of vitexin in oxidative stress-related diseases. *Food Sci. Nutr.* 8(6), 2569-2580.
- Bagdas, D., Etoz, B.C., Gul, Z., Ziyankok, S., Inan, S., Turacozen, O., Gul, N.Y., Topal, A., Cinkilic, N., Tas, S., Ozyigit, M.O., Gurun, M.S., 2015. *In vivo* systemic chlorogenic acid therapy under diabetic conditions: Wound healing effects and cytotoxicity/genotoxicity profile. *Food Chem. Toxicol.* 81, 54-61.
- Barmaverain, D., Hasler, S., Kalbermatten, C., Plath, M., Kalbermatten, R., 2022. Oxidation during fresh plant processing: A race against time. *Processes* 10, 1335.
- Bhavna, D., Souravh, B., Naresh, S.G., 2017. A review on quinic acid and its therapeutic potential. *Inventi Rapid: Mol. Pharmacol.* 3, 1-6.
- Chen, L.Y., Huang, C.N., Liao, C.K., Chang, H.M., Kuan, Y.H., Tseng, T.J., Yen, K.J., Yang, K.L., Lin, H.C., 2020. Effects of rutin on wound healing in hyperglycemic rats. *Antioxidants (Basel)* 9(11), 1122.
- DeRango-Adem, E.F., Blay, J., 2021. Does oral apigenin have real potential for a therapeutic effect in the context of human gastrointestinal and other cancers?. *Front. Pharmacol.* 12, 681477.
- Djamila, B., Eddine, L.S., Abderrhmane, B., 2022. *In vitro* antioxidant activities of copper mixed oxide (CuO/Cu<sub>2</sub>O) nanoparticles produced from the leaves of *Pheonix dactylifera* L. *Biomass Convers. Biorefin.* <https://doi.org/10.1007/s13399-022-02743-3>.
- Erdogan, T., Gonenc, T., Cakilcioglu, U., Kivcak, B., 2014. Fatty acid composition of the aerial parts of some *Centaurea* species in Elazig, Turkey. *Trop. J. Pharm. Res.* 13(4), 613-616.
- Essien, E.R., Atasie, V.N., Oyebanji, T.O., Nwude, D.O., 2020. Biomimetic synthesis of magnesium oxide nanoparticles using *Chromolaena odorata* (L.) leaf extract. *Chem. Pap.* 74(7), 2101-2109.
- Eze, F.N., Jayeoye, T.J., 2021. *Chromolaena odorata* (Siam weed): A natural reservoir of bioactive compounds with potent anti-fibrillogenic, antioxidative, and cytocompatible properties. *Biomed. Pharmacother.* 141, 111811.
- Eze, F.N., Tola, A.J., 2020. Protein glycation and oxidation inhibitory activity of *Centella asiatica* phenolics (CAP) in glucose-mediated bovine serum albumin glycoxidation. *Food Chem.* 332, 127302.
- Gaba, S., Rai, A.K., Varma, A., Prasad, R., Goel, A., 2022. Biocontrol potential of mycogenic copper oxide nanoparticles against *Alternaria brassicae*. *Front Chem.* 10, 966396.
- Genc, S., Cicek, B., Yeni, Y., Hacimuftuoglu, A., 2022. Wound healing potential of quinic acid in human dermal fibroblasts by regulating the expression of FN1 and COL1 $\alpha$  genes. *Turk. J. Nat. Sci.* 11(4), 63-69.
- Gudimella, K.K., Gedda, G., Kumar, P.S., Babu, B.K., Yamajala, B., Rao, B.V., Singh, P.P., Kumar, D., Sharma, A., 2022. Novel synthesis of fluorescent carbon dots from bio-based *Carica papaya* leaves: Optical and structural properties with antioxidant and anti-inflammatory activities. *Environ. Res.* 204, 111854.
- Güler, O., Polat, R., Karakose, M., Cakilcioglu, U., Akbulut, S., 2021. An ethnoveterinary study on plants used for the treatment of livestock diseases in the province of Giresun (Turkey). *S. Afr. J. Bot.* 142(8), 53-62.
- Hajizadeh, Y.S., Harzandi, N., Babapour, E., Yazdani, M., Ranjbar, R., 2022. Green synthesis and characterization of copper nanoparticles using Iranian *Propolis* extracts. *Adv. Mater. Sci. Eng.* Article ID:8100440. <https://doi.org/10.1155/2022/8100440>.
- Hong, R., Kang, T.Y., Michels, C.A., Gadura, N., 2012. Membrane lipid peroxidation in copper alloy-mediated contact killing of *Escherichia coli*. *Appl. Environ. Microbiol.* 78(6), 1776-1784.
- Hsu, C.Y., Chan, Y.P., Chang, J., 2007. Antioxidant activity of extract from *Polygonum cuspidatum*. *Biol. Res.* 40(1), 13-21.
- Huang, M., Cao, X., Zhang, J., Liu, H., Lu, J., Yi, D., Ma, Y., 2022. Mesosphere of carbon-shelled copper nanoparticles with high conductivity and thermal stability via direct carbonization of polymer soft templates. *Materials* 15(21), 7536.
- Jagatheesh, S., Anandhi, D., Revathi, K., Sundaravalli, K., Jasmin Vigila, J., Devi, R., 2020. Biological potential and characterization of green synthesized silver nanoparticles using *Chromolaena odorata* (Linn). *Ann. Rom. Soc. Cell Biol.* 24 (1), 227-238.
- Jayeoye, T.J., Eze, F.N., Olatunde, O.O., Benjakul, S., Rujiralai, T., 2021. Synthesis of silver and silver@zerovalent iron nanoparticles using *Chromolaena odorata* phenolic extract for antibacterial activity and hydrogen peroxide detection. *J. Environ. Chem. Eng.* 9(3), 105224.
- Kausar, H., Mehmood, A., Khan, R.T., Ahmad, K.S., Hussain, S., Nawaz, F., Iqbal, M.S., Nasir, M., Ullah, T.S., 2022. Green synthesis and characterization of copper nanoparticles for investigating their effect on germination and growth of wheat. *PLoS One* 17(6), e0269987.
- Kazemina, M., Mehrabi, A., Mahmoudi, R., 2022. Chemical composition, biological activities, and nutritional application of Asteraceae family herbs: A systematic review. *Trends Phytochem. Res.* 6(3), 187-213.
- Khatun, S., Chatterjee, N.C., Cakilcioglu, U., 2011. Antioxidant activity of the medicinal plant *Coleus forskohlii* Briq. *Afr. J. Biotechnol.* 10(13), 2530-2535.
- Kota, S., Dumpala, P., Anantha, R., Verma, M., Kandepu, S., 2017. Evaluation of therapeutic potential of the silver/silver chloride nanoparticles synthesized with the aqueous leaf extract of *Rumex acetosa*. *Sci Rep.* 7,

11566.

- Kota, S., Dumpala, P., Dachehalli, H.P., Ratna Kumari, A., 2018. Understanding the phytochemical constitution, antioxidant potential and spectral characteristics of aqueous extracts of the chosen leafy vegetables from south India. *Trends Phytochem. Res.* 2(2), 111-118.
- Kota, S., Govada, V.R., Anantha, R.K., Verma, M.K., 2017. An investigation into phytochemical constituents, antioxidant, antibacterial and anti-cataract activity of *Alternanthera sessilis*, a predominant wild leafy vegetable of South India. *Biocatal. Agric. Biotechnol.* 10(2), 197-203.
- Kumar, B.V., Reddy, K.H., 2022. Green synthesis, characterization and antimicrobial activity of nanosized cuprous oxide fabricated using aqueous extracts of *Allium cepa* and *Raphanus sativus*. *Int. J. Nano Dimens.* 13(2), 214-226.
- Lo, S., Leung, E., Fedrizzi, B., Barker, D., 2021. Syntheses of mono-acylated luteolin derivatives, evaluation of their anti-proliferative and radical scavenging activities and implications on their oral bioavailability. *Sci. Rep.* 11(1), 12595.
- Luo, H., Yamamoto, Y., Kim, J.A., Jung, J.S., Koh, Y.J., Hur, J.S., 2009. Lecanoric acid, a secondary lichen substance with antioxidant properties from *Umbilicaria antarctica* in maritime Antarctica (King George Island). *Polar Biol.* 32(7), 1033-1040.
- Ma, Y., Hao, G., Lin, X., Zhao, Z., Yang, A., Cao, Y., Zhang, S., Fan, L., Geng, J., Zhang, Y., Chen, J., Song, C., He, M., Du, H., 2022. Morroniside protects human granulosa cells against H<sub>2</sub>O<sub>2</sub>-induced oxidative damage by regulating the Nrf2 and MAPK signaling pathways. *Evid. Based Complement. Alternate Med. (eCAM)* 8099724.
- Macedo, D.C.S., Almeida, F.J.F., Wanderley, M.S.O., Ferraz, M.S., Santos, N.P.S., Lopez, A.M.Q., Santos-Magalhaes, N.S., Lira-Nogueira, M.C.B., 2021. Usnicacid: From an ancient lichen derivative to promising biological and nanotechnology applications. *Phytochem. Rev.* 20(4), 609-630.
- Madiha, B., Zahid, Q., Farwa, H., Nida, M., 2018. Biosynthesis of copper nanoparticles by using *Aloe barbadensis* leaf extracts. *Inter. Ped. Dent. Open Acc. J.* 1(2), 000110.
- Mahdavi, B., Hosseini, S., Mohammadhosseini, M., Mehrshad, M., 2022. Preparation and characterization of a novel magnetized nanosphere as a carrier system for drug delivery using *Plantago ovata* Forssk. hydrogel combined with mefenamic acid as the drug model. *Arabian J. Chem.* 15(10), 104128.
- Mobarak, M.B., Hossain, M.S., Chowdhury, F., Ahmed, S., 2022. Synthesis and characterization of CuO nanoparticles utilizing waste fish scale and exploitation of XRD peak profile analysis for approximating the structural parameters. *Arab. J. Chem.* 15(10), 104117.
- Morey, M., O'Gaora, P., Pandit, A., Helary, C., 2019. Hyperglycemia acts in synergy with hypoxia to maintain the pro-inflammatory phenotype of macrophages. *PLoS One* 14(8), e0220577.
- Moroz, A., Deffune, E., 2013. Platelet-rich plasma and chronic wounds: Remaining fibronectin may influence matrix remodeling and regeneration success. *Cytotherapy* 15(11), 1436-1439.
- Munira, M., Rasidah, Zakiah, N., Nasir, M., 2022. Identification of chemical compounds and antibacterial activity test of Kirinyuh leaf extract (*Chromolaena odorata* L.) from *le Seum* geothermal area, Regency of Aceh Besar, Indonesia. *Rasayan J. Chem.* 15(4), 2852-2857.
- Nguyen, D.T., Duong, N.L., Nguyen, V.M., Thi Luong, C.V., Nguyen, P.A., Nguyen, T., 2020. *Chromolaena odorata* extract as a green agent for the synthesis of Ag@AgCl nanoparticles inactivating bacterial pathogens. *Chem. Pap.* 74(6), 1849-1857.
- Panche, A.N., Diwan, A.D., Chandra, S.R., 2016. Flavonoids: An overview. *J. Nutr. Sci.* 5, e47.
- Pandith, H., Zhang, X., Thongpraditchote, S., Wongkrajang, Y., Gritsanapan, W., Baek, S.J., 2013. Effect of siam weed extract and its bioactive component scutellarein tetramethyl ether on anti-inflammatory activity through NF- $\kappa$ B pathway. *J. Ethnopharmacol.* 147(2), 434-41.
- Pestryakov, A.N., Petranovskii, V.P., Kryazhov, A., Ozhereliev, O., Pfander, N., Knop-Gericke, A., 2004. Study of copper nanoparticles formation on supports of different nature by UV-Vis diffuse reflectance spectroscopy. *Chem. Phys. Lett.* 385(3-4), 173-176.
- Phan, T.T., Hughes, M.A., Cherry, G.W., 1998. Enhanced proliferation of fibroblasts and endothelial cells treated with an extract of the leaves of *Chromolaena odorata* (Eupolin), an herbal remedy for treating wounds. *Plast. Reconstr. Surg.* 101(3), 756-65.
- Phan, T.T., Wang, L., See, P., Grayer, R.J., Chan, S.Y., Lee, S.T., 2001. Phenolic compounds of *Chromolaena odorata* protect cultured skin cells from oxidative damage: Implication for cutaneous wound healing. *Biol. Pharm. Bull.* 24(12), 1373-1379.
- Polat, R., Çakılcıoğlu, U., Selvi S., Türkmen Z., Kandemir, A., 2017. The anatomical and micromorphological properties of three endemic and medicinal *Salvia* species (Lamiaceae) in Erzincan (Turkey). *Plant Biosys.* 151 (1), 63-73.
- Raaman, N., 2006. *Phytochemical Techniques*. New India Publishing Agency, New Delhi, India.
- Sirinthipaporn, A., Jiraungkoorskul, W., 2017. Wound healing property review of Siam weed, *Chromolaena odorata*. *Pharmacogn. Rev.* 11(21), 35-38.
- Slavin, Y.N., Asnis, J., Hafeli, U.O., Bach, H., 2017. Metal nanoparticles: Understanding the mechanisms behind antibacterial activity. *J. Nanobiotechnol.* 15(1), 1-20.
- Smart-Dre-M: Biopolymer Composite-Based Nano-Fibrous Wound Dressing Material, Indian Patent No. 202041052202; Published on 12.12.2020.
- Tabrez, S., Khan, A.U., Mirza, A.A., Suhail, M., Jabir, N.R., Zughibi, T.A., Alam, M., 2022. Biosynthesis of copper oxide nanoparticles and its therapeutic efficacy against colon cancer. *Nanotechnol. Rev.* 11(1), 1322-1331.
- Thang, P.T., Patrick, S., Teik, L.S., Yung, C.S., 2001. Antioxidant effects of the extracts from the leaves of *Chromolaena odorata* on human dermal fibroblasts and epidermal keratinocytes against hydrogen peroxide and hypoxanthine-xanthine oxidase induced damage. *Burns* 27(4), 319-327.
- Tungmunthum, D., Thongboonyou, A., Pholboon, A., Yangsabai, A., 2018. Flavonoids and other phenolic compounds from medicinal plants for pharmaceutical and medical aspects: An overview. *Medicines (Basel)*



5(3), 93.

Vane, J.R., Botting, R.M., 1995. New insights into the mode of action of anti-inflammatory drugs. *Inflamm. Res.* 44(1), 1-10.

Vijayakumar, G., Kesavan, H., Kannan, A., Arulanandam, D., Kim, J.H., Kim, K.J., Song, H.J., Kim, H.J., Rangarajulu, S.K., 2021. Phytosynthesis of copper nanoparticles using extracts of spices and their antibacterial properties. *Processes* 9(8), 1341.

Vitalini, S., Iriti, M., Puricelli, C., Ciuchi, D., Segale, A., Fico, G., 2013. Traditional knowledge on medicinal and food plants used in Val San Giacomo (Sondrio, Italy)-An Alpine ethnobotanical study. *J. Ethnopharmacol.* 145(2), 517-529.

Vitalini, S., Tomè, F., Fico, G., 2009. Traditional uses of medicinal plants in Valvestino (Italy). *J. Ethnopharmacol.* 121 (1), 106-116.

Wang, W., Huang, W., Li, L., Ai, H., Sun, F., Liu, C., An, Y., 2008. Morroniside prevents peroxide-induced apoptosis by induction of endogenous glutathione in human neuroblastoma cells. *Cell. Mol. Neurobiol.* 28(2), 293-305.

Wongkrajang, Y., Thongpraditchote, S., Nakornchai, S., Chuakul, W., Muangklum, K., Jaiarj, P., 1994. Hemostatic activities of *Eupatorium odoratum* Linn.: Calcium removal extract. *Mahidol University J. Pharma Sci.* 21, 143-148.

Zhang, Y., Mahdavi, B., Mohammadhosseini, M., Rezaei-Seresht, E., Paydarfard, S., Qorbani, M., Karimian, M., Abbasi, N., Ghaneialvar, H., Karimi, E., 2021. Green synthesis of NiO nanoparticles using *Calendula officinalis* extract: Chemical characterization, antioxidant, cytotoxicity, and anti-esophageal carcinoma properties. *Arabian J. Chem.* 14(10), 103105.